



OPEN ACCESS

EDITED BY

Jinseok Lee,
Kyung Hee University, South Korea

REVIEWED BY

Mohamed Abdelazez,
Carleton University, Canada
Chenxi Yang,
Southeast University, China

*CORRESPONDENCE

Van-Khoa D. Le,
khoaldv@oucru.org

SPECIALTY SECTION

This article was submitted to
Computational Physiology and
Medicine,
a section of the journal
Frontiers in Physiology

RECEIVED 16 August 2022

ACCEPTED 07 October 2022

PUBLISHED 11 November 2022

CITATION

Le V-KD, Ho HB, Karolcik S,
Hernandez B, Greeff H, Nguyen VH,
Phan NQK, Le TP, Thwaites L,
Georgiou P and Clifton D (2022),
vital_sqi: A Python package for
physiological signal quality control.
Front. Physiol. 13:1020458.
doi: 10.3389/fphys.2022.1020458

COPYRIGHT

© 2022 Le, Ho, Karolcik, Hernandez,
Greeff, Nguyen, Phan, Le, Thwaites,
Georgiou and Clifton. This is an open-
access article distributed under the
terms of the [Creative Commons
Attribution License \(CC BY\)](#). The use,
distribution or reproduction in other
forums is permitted, provided the
original author(s) and the copyright
owner(s) are credited and that the
original publication in this journal is
cited, in accordance with accepted
academic practice. No use, distribution
or reproduction is permitted which does
not comply with these terms.

vital_sqi: A Python package for physiological signal quality control

Van-Khoa D. Le^{1*}, Hai Bich Ho¹, Stefan Karolcik²,
Bernard Hernandez², Heloise Greeff³, Van Hao Nguyen⁴,
Nguyen Quoc Khanh Phan¹, Thanh Phuong Le¹,
Louise Thwaites¹, Pantelis Georgiou² and David Clifton³
on behalf of the Vietnam ICU Translational Applications
Laboratory (VITAL) Investigators

¹Oxford University Clinical Research Unit, Ho Chi Minh City, Vietnam, ²Department of Electrical and Electronic Engineering, Imperial College London, South Kensington Campus, London, United Kingdom, ³Department of Engineering Science, Institute of Biomedical Engineering, University of Oxford, Oxford, United Kingdom, ⁴Hospital of Tropical Diseases, University of Medicine and Pharmacy, Ho Chi Minh City, Vietnam

Electrocardiogram (ECG) and photoplethysmogram (PPG) are commonly used to determine the vital signs of heart rate, respiratory rate, and oxygen saturation in patient monitoring. In addition to simple observation of those summarized indexes, waveform signals can be analyzed to provide deeper insights into disease pathophysiology and support clinical decisions. Such data, generated from continuous patient monitoring from both conventional bedside and low-cost wearable monitors, are increasingly accessible. However, the recorded waveforms suffer from considerable noise and artifacts and, hence, are not necessarily used prior to certain quality control (QC) measures, especially by those with limited programming experience. Various signal quality indices (SQIs) have been proposed to indicate signal quality. To facilitate and harmonize a wider usage of SQIs in practice, we present a Python package, named vital_sqi, which provides a unified interface to the state-of-the-art SQIs for ECG and PPG signals. The vital_sqi package provides with seven different peak detectors and access to more than 70 SQIs by using different settings. The vital_sqi package is designed with pipelines and graphical user interfaces to enable users of various programming fluency to use the package. Multiple SQL extraction pipelines can take the PPG and ECG waveforms and generate a bespoke SQL table. As these SQL scores represent the signal features, they can be input in any quality classifier. The package provides functions to build simple rule-based decision systems for signal segment quality classification using user-defined SQL thresholds. An experiment with a carefully annotated PPG dataset suggests thresholds for relevant PPG SQIs.

KEYWORDS

signal quality index, electrocardiogram, photoplethysmogram, vital signs, continuous monitoring, open-source, Python toolbox



开放获取

编辑
Jinseok Lee, 韩国庆熙大学审查
Mohamed Abdelazez,
加拿大卡尔顿大学
杨晨曦：
中国东南大学
范科阿勒，
khoaldv@oucru.org专业部分
本文交给
计算生理学和
医学，
杂志的一部分
Frontiers in Physiology2022年8月16日收到
接受日期：2022年10月7日
发布日期2022年11月11日引文
Le V-KD, Ho HB, Karolcik S、埃尔南德斯B、Greeff H、Nguyen VH、Phan NQK、Le TP、Thwaites L、Georgiou P和克利夫顿D (2022), vital_sqi: 用于生理信号质量控制的Python包。前面生理学13: 1020458。
doi: 10.3389/fphys.2022.1020458版权
© 2022 Le, Ho, Karolcik, 埃尔南德斯, Greeff, Nguyen, Phan, Le, Thwaites, Georgiou and 克利夫顿。这是一篇开放存取的文章，根据知识共享署名许可证（CC BY）的条款分发。允许在其他论坛使用、分发或复制，前提是注明原作者和版权所有者，并根据公认的学术惯例引用本期刊的原始出版物。不允许在不遵守这些条款的情况下使用、分发或复制。

vital_sqi: 用于生理信号质量控制的Python包

范科阿Le *、Hai Bich Ho、Stefan Karolcik、Bernard埃尔南德斯、Heloise Greeff、货车Hao Nguyen、Nguyen Quoc Khanh Phan、Thanh Chongong Le、Louise Thwaites、Pantelis Georgiou和大卫克利夫顿代表越南ICU转化应用实验室（VITAL）研究者

1牛津大学临床研究单位，越南胡志明市，英国伦敦帝国理工学院电气和电子工程系，英国伦敦南肯辛顿校区，英国牛津大学生物医学工程研究所工程科学系，英国牛津，越南胡志明市医药大学热带病医院

心电图（ECG）和光电容积描记图（PPG）通常用于确定患者监测中的心率、呼吸率和氧饱和度的生命体征。除了简单观察这些汇总指标外，还可以分析波形信号，以提供对疾病病理生理学的更深入了解并支持临床决策。从传统床边和低成本可穿戴监测器的连续患者监测产生的此类数据越来越容易获得。然而，所记录的波形遭受相当大的噪声和伪影，并且因此不一定在某些质量控制（QC）措施之前使用，特别是对于那些具有有限编程经验的人。已经提出了各种信号质量指数（SQI）来指示信号质量。为了促进和协调SQI在实践中的更广泛使用，我们提出了一个Python包，名为vital_sqi，它提供了一个统一的接口，以最先进的SQI的ECG和PPG信号。vital_sqi软件包提供了七种不同的峰值检测器，并通过使用不同的设置访问70多个SQI。vital_sqi包设计有管道和图形用户界面，以使各种编程流畅度的用户能够使用该包。多个SQI提取管道可以获取PPG和ECG波形并生成定制的SQI表。由于这些SQI分数代表信号特征，因此它们可以输入任何质量分类器。该软件包提供了使用用户定义的SQI阈值构建简单的基于规则的信号段质量分类决策系统的功能。使用仔细注释的PPG数据集的实验建议了相关PPG SQI的阈值。

关键词

信号质量指数, 心电图, 光电容积描记图, 生命体征, 连续监测, 开源, Python工具箱

1 Introduction

Continuous monitoring in ambulatory (Sana et al., 2020) and limited-resourced settings (Nantume et al., 2021) with medical-grade wearables is becoming increasingly widespread as increasing numbers of low-cost devices are available to provide continuously streamed data for long periods of time. Conventionally, physiological signals are recorded continuously for hours, but only the numerals, i.e., the summarized numbers, are reported and used in most analyses. Although powerful insights into disease processes and prognosis have been gained from such methodology, deeper understanding could also be learnt from the signal waveforms themselves as they contain significantly greater information concerning the underlying cardiovascular physiology. Machine-learning and deep-learning technologies now provide us with the ability to analyze these complex waveform data and, hence, the potential to use the electrocardiogram (ECG) and photoplethysmogram (PPG) waveforms to provide pathophysiological insights (Becker, 2006; Elgendi, 2012; Pereira et al., 2020), predict disease progression (Tadesse et al., 2020; Akbilgic et al., 2021; Raghunath et al., 2020), or detect abnormality (Badawi et al., 2021). Analysis of data from low-cost wearable devices, especially in ambulatory patients, can be limited by poor signal quality and noise. Simple-to-use tools to evaluate quality and select appropriate data for analysis are required in order to optimize the potential for devices in improving patient outcomes.

The ECG represents the heart's electrical activity, transmitted through the body and recorded by electrodes placed on the skin of the torso and limbs. The resulting pattern consists of a baseline and waves, i.e., positive and negative deflections from the baseline depending on depolarization and repolarization activity in the heart. These deflections are named as the P wave, QRS complex (Q wave, R wave, and S wave), and T wave. The PPG records the changes in peripheral blood volume, also in the waveform pattern, by measuring the light intensity (through or reflected) using a sensor placed on the skin of various body parts such as the ear or fingertip. The PPG waveform contains a pulsatile ("AC") component attributed to change of blood volume with each heartbeat and a baseline component ("DC") varying at low frequency attributed to autonomic nervous system activity. Both ECG and PPG, recorded by either bedside monitors or low-cost wearable devices, are prone to noise and artifacts. The main causes can be categorized as physiological, (e.g., skin movement or muscle contraction) and non-physiological (e.g., ongoing electrical stimuli, device displacement or signal loss due to Bluetooth disconnection) (Nagai et al., 2017; Lee et al., 2020; Pollreisz, 2022; Seok et al., 2021). In our experience using both finger tip oximeter and patch ECG monitor, loose sensor contact and Bluetooth disconnection, are among the most

frequent causes. The timely identification of noisy segments is essential for both monitoring and downstream analyses.

Although many signal quality indices (SQIs) and methodologies have been reported for both PPG and ECG (refer to Table 1), an open-source unified access to a wide range of SQIs does not exist yet. In addition, a powerful toolbox such as the Cardiovascular Signal Toolbox published in PhysioNet is only released in MATLAB. Furthermore, the Toolbox's scope does not concentrate on deriving the SQI scores but extracting features for analysis.

Thus these challenges have provided the motivation for the development of a SQI package that allows multiple options for practitioners, especially in Python. The package we have developed concentrates on the assessment of signal quality. Consequently our work increases the available tools for computing SQI. In addition, the SQI is well-categorized into specific groups. We also design a simple user interface for non-expert practitioners to select their preferred settings. In this study, we focus on the ECG and PPG waveforms derived from wearable devices, where noise and artifact are likely to be highest.

For automated signal quality control, we implemented the 74 state-of-the-art SQIs in a lightweight open-source Python package called `vital_sqi`. The package is used to help researchers obtain signals suitable for analysis of HRV and training of machine-learning models. The package also provides pipelines to execute end-to-end SQI extraction and classification and graphical user interfaces (GUIs) for users of different programming fluency.

2 The `vital_sqi` package

2.1 Installation and requirements

The package is built for Python 3.7 and 3.8, which is released through PyPi, and it can be installed through Python Package Manager PIP. The requirements include a number of popular Python packages such as NumPy, Pandas, and SciPy for signal processing; pyEDFlib and WFDB for reading/writing waveform formats such as "EDF" and "MIT ([Physio.net](#)).". We also inherit R-peak detection and heart rate variability (HRV) computation from py-ecg-detectors, HRV analysis (Champseix et al., 2018), and HeartPy (van Gent et al., 2019). Further installation instruction and requirements can be found in the source at GitHub and the documentation at Read the Docs.

2.2 Structure and modules

The package is structured as a combination of modules for different functionalities as shown in Figure 1. The main workflow contains three steps: data preprocessing, SQI computation, and

引言门诊连续监测 (Sana 等人, 2020) 和资源有限的环境 (Nantume 等人, 随着越来越多的低成本设备可用于长时间提供连续流式数据, 医疗级可穿戴设备的应用正变得越来越普遍。传统上, 生理信号被连续记录数小时, 但仅记录数字, 即, 在大多数分析中报告和使用了汇总的数字。虽然已经从这种方法中获得了对疾病过程和预后的强大见解, 但也可以从信号波形本身中获得更深入的理解, 因为它们包含有关潜在心血管生理学的更多信息。机器学习和深度学习技术现在为我们提供了分析这些复杂波形数据的能力, 因此, 有可能使用心电图 (ECG) 和光电容积描记图 (PPG) 波形来提供病理生理学见解 (Becker, 2006; Elgendi, 2012; 佩雷拉等人, 2020), 预测疾病进展 (Tadesse 等人, 2020; Akbilgic 等人, 2021; Raghunath 等人, 2020), 或检测异常 (Badawi 等人, 2021 年)。低成本可穿戴设备的数据分析, 特别是在非卧床患者中, 可能会受到信号质量差和噪声的限制。需要使用简单易用的工具来评估质量并选择适当的数据进行分析, 以优化器械在改善患者结局方面的潜力。

ECG 代表心脏的电活动, 通过身体传输并由放置在躯干和四肢皮肤上的电极记录。所得到的图案由基线和波组成, 即, 根据心脏中的去极化和复极化活动, 从基线的正向和负向偏转。这些偏转被称为P波、QRS波群 (Q波、R波和S波) 和T波。PPG通过使用放置在诸如耳朵或指尖的各种身体部位的皮肤上的传感器测量光强度 (通过或反射) 来记录外周血容量的变化, 也以波形模式记录。PPG波形包含归因于随着每次心跳的血容量变化的脉动 (“AC”) 分量和归因于自主神经系统活动的在低频下变化的基线分量 (“DC”)。由床边监护仪或低成本可穿戴设备记录的ECG 和 PPG都容易产生噪声和伪影。主要原因可以分为生理性 (例如, 皮肤运动或肌肉收缩) 和非生理 (例如, 持续的电刺激、设备位移或由于蓝牙断开而导致的信号丢失) (永井等人, 2017; Lee 等人, 2020; Pollreisz, 2022; Seok 等人, 2021 年)。在我们使用指尖血氧仪和贴片ECG 监测仪的经验中, 传感器接触松动和蓝牙断开

是最常见的原因。噪声段的及时识别对于监测和下游分析都是必不可少的。

尽管已经报告了PPG和ECG 的许多信号质量指数 (SQI) 和方法 (参见表1), 但尚不存在对各种SQI的开源统一访问。此外, 功能强大的工具箱 (如PhysioNet上发布的Cardiovascular Signal Toolbox) 仅在MATLAB中发布。此外, SQI的范围并不集中于导出SQI分数, 而是提取用于分析的特征。

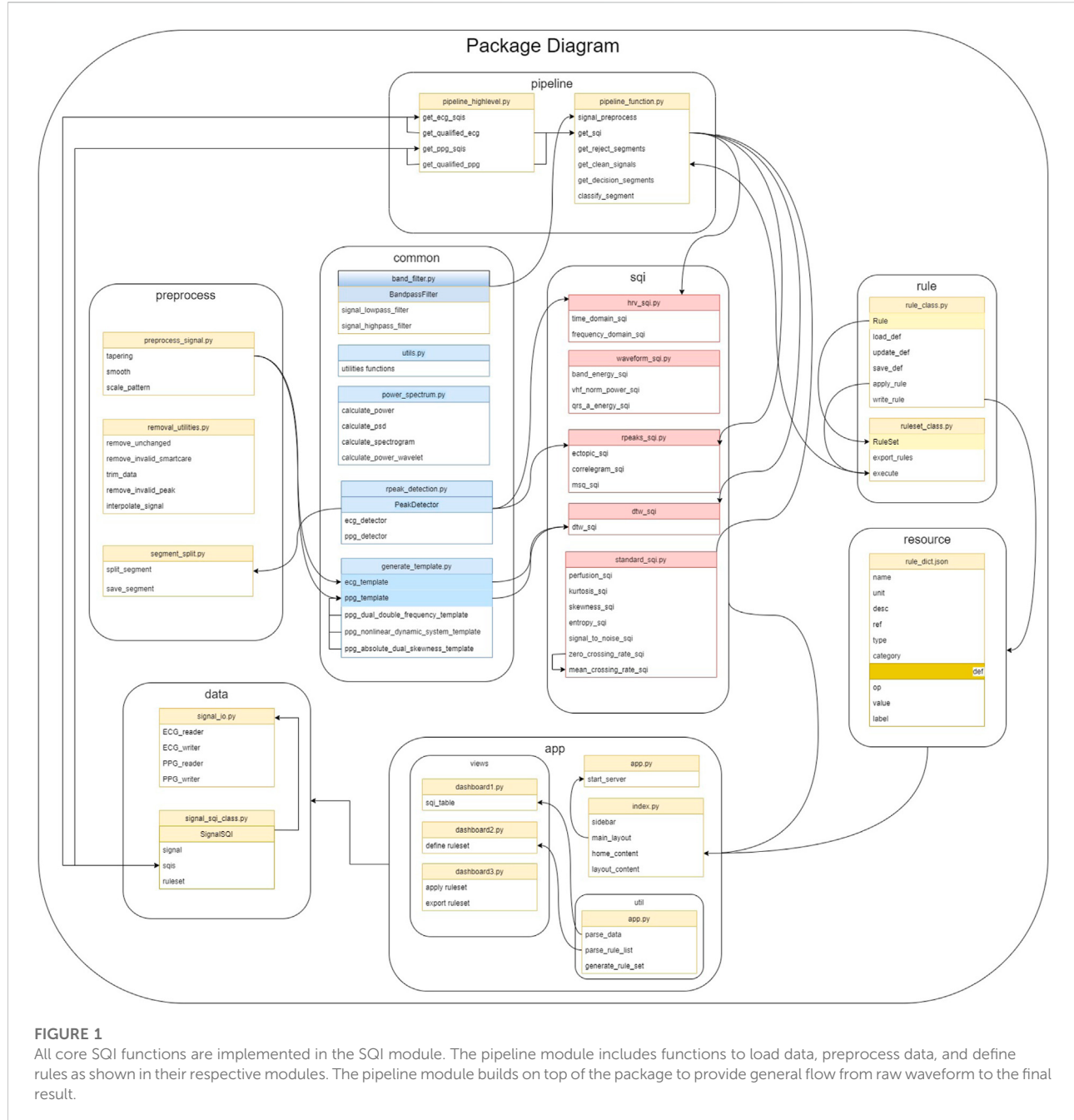
因此, 这些挑战为开发SQI包提供了动力, 该包允许实践者有多种选择, 特别是在Python中。我们开发的软件包集中于信号质量的评估。因此, 我们的工作增加了计算SQI的可用工具。此外, SQI被很好地分类为特定的组。我们还设计了一个简单的用户界面, 为非专业从业人员选择他们的首选设置。在这项研究中, 我们专注于来自可穿戴设备的ECG 和PPG波形, 其中噪声和伪影可能最高。

为了实现自动信号质量控制, 我们在一个名为vital_sqi的轻量级开源Python包中实现了74个最先进的SQI。该软件包用于帮助研究人员获得适合分析HRV和训练机器学习模型的信号。该软件包还提供了管道来执行端到端的SQI提取和分类, 并为不同编程流畅度的用户提供图形用户界面 (GUI)。

2 vital_sqi包

2.1 安装和要求该包是为Python 3.7 和3.8 构建的, 通过PyPi发布, 可以通过Python 包管理器PIP安装。需求包括许多流行的Python 包, 如用于信号处理的NumPy、Pandas 和SciPy ;用于阅读/写入波形格式的pyEDFlib 和WFDB, 如“EDF”和“MIT (Physio .net)” 。我们还从py-ecg-detectors 、HRV分析 (Champseix 等人, 2018) 和HeartPy (货车Gent 等人, 2019 年)。进一步的安装说明和要求可以在GitHub 的源代码和阅读文档中找到。

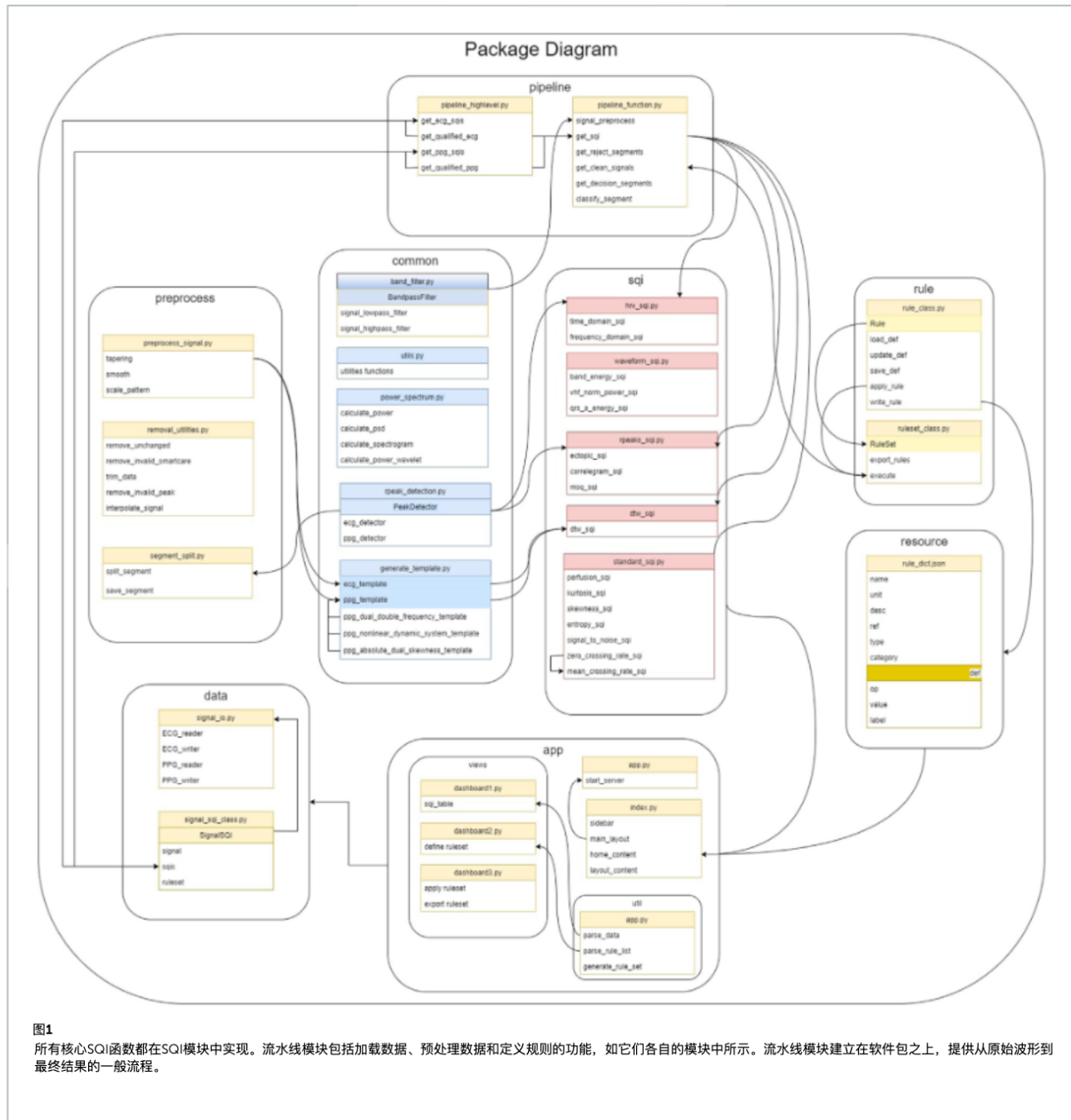
2.2 如图1所示, 软件包的结构是由不同功能的模块组合而成的。主要工作流程包含三个步骤: 数据预处理、SQI计算和



rule-based decision of signal quality. The modules are designed corresponding to these steps. At any step, the users can introduce results from external computation to use within vital_sqi. To further facilitate flexible use, we provide access to these modules individually and complete pipelines from raw waveform to either 1) SQI table or 2) signal quality classification. All parameters of SQI extraction functions and those of the rule-based classification are configurable through SQI and rule dictionaries in the JSON format, allowing clear organization when running quality control experiments.

At the core of the package is the SQI module, in which the 74 selected SQIs are divided into four groups (details in [Section 2.3](#)):

- Statistical SQIs such as kurtosis, skewness, and entropy.
- Heart rate variability (HRV)-based SQIs such as SDNN, SDSD, and RMSSD.
- RR interval-based SQIs such as ectopic, correlogram, and MSQ.
- Waveform-based SQIs such as DTW, qrs_energy, and qrs_a.



基于规则的信号质量决策。模块设计与这些步骤相对应。在任何步骤中，用户都可以引入外部计算的结果，以便在vital_squi中使用。为了进一步方便灵活使用，我们提供对这些模块的单独访问，并提供从原始波形到1) SQI表或2) 信号质量分类的完整管道。SQI提取函数和基于规则的分类的所有参数都可以通过JSON格式的SQI和规则字典进行配置，从而在运行质量控制实验时实现清晰的组织。

软件包的核心是SQI模块，其中74个选定的SQI分为四组（详见第2.3节）：

- 统计SQI，如峰度、偏度和熵。
- 基于心率变异性（HRV）的SQI，如SDNN、SDSD和RMSSD。
- 基于RR间期的SQI，如异位、相关图和MSQ。
- 基于波形的SQI，如DTW、qrs_energy和qrs_a。

The usage is built around three classes in *data* and *rule* modules.

- Signal SQI object has attributes for the raw signal, SQI table, and rule-based classification setup. The object is initialized by reading waveforms and is updated at each step.
- Rule object is constructed for each SQI with user-defined thresholds to classify a signal segment as ‘accept’ or ‘reject.’ A number of rule objects are initialized by reading in SQI dictionary from a JSON file.
- Ruleset is a group of rule objects to be executed in order on the extracted SQI table. It is a lightweight, yet efficient, approach to signal quality classification (shown in our experiments in 3.5). The ruleset object is also initialized from a JSON file. Templates of these JSON configuration files, with our recommended thresholds, are provided in the *resource* module.

The two modules of *Preprocess* and *Common* feature share supporting functions to prepare the signal for SQI extraction such as filtering, trimming, or R-peak detection. Last, we provide a web-based GUI, which can easily be used to construct rule and ruleset and execute them on an input SQI table. Coupled with the provided pipelines in the *Pipeline* module for SQI extraction, this *Application* module allows users to quickly obtain quality indices and separate accepted and rejected signal segments.

2.3 Signal quality indices

Aiming to separate usable from unusable signal segments, the SQIs implemented in this work have been selected to allow flexible usage, suitable for classification of signals both before and after preprocessing. Therefore, the first step is signal segmentation either by signal duration or by beat, i.e., each segment is equivalent to a cycle (PPG) or QRS complex (ECG). The package features seven peak detectors as shown in Table 2.3.1. The available SQIs are divided into four categories, corresponding to four modules as explained later.

2.3.1 Peak detectors

A total of seven different peak detectors are available for selection when processing data using the *vital_sqi* package. These are briefly summarized in the table as follows:

Users are encouraged to experiment with different peak detectors when working with a particularly noisy datasets. The performance of each detector is influenced by the type and extent of prior preprocessing of the dataset.

Algorithm ID	Peak detector name	Input parameter	Source
1	Adaptive threshold		Shin et al. (2009)
2	Count origin		Schäfer and Kratky (2008)
3	Clustering		
4	Slope sum		Zong et al. (2003)
5	Moving average		Elgendi et al. (2013)
6	Default SciPy		Virtanen et al. (2020)
7	Billauer algorithm		Billauer (2009)

2.3.2 Statistical SQIs

Statistical SQIs analyze the signal trends within the segment, providing features of the underlying probability distribution. The implemented SQIs were built on the previous work of Elgendi (2016). The utilization of statistical SQIs to determine PPG signal quality has been significantly researched in the last decade, showing promising performance when distinguishing between the acceptable and unfit signal segments (Selvaraj et al., 2011; Krishnan et al., 2010; Elgendi, 2016). Combining the statistical SQIs with other SQIs provided in this package further improves their cited performance and allows researchers to fine-tune their signal quality selection criteria. For the full list of available statistics-based SQIs, refer to Table 1.

2.3.3 Heart rate variability-based and RR interval-based SQIs

In other modes of operation, the accuracy to identify serial R waves (for ECG) or systolic peaks (PPG) within the signal is examined. RR interval-based SQIs obtain consensus between different methods of detecting RR peaks.

Beyond pure SQI calculation, the HRV indices are calculated from the RR signal, which can allow inference regarding the functionality and control of the heart and nervous system. Using the package, HRV is derived by a sequence of processes: filtering, resampling, peak detection, removing false peaks, and extracting features. These steps are necessary as poor signal quality can lead to inaccurate labeling of R waves and inaccurate HRV indices. Specifically, HRV features in the frequency domain and time domain are distinguishable between normal and ill patient and non-observable in human, which refers to bad quality.

2.3.4 Waveform-based SQIs

In computing these indices, the signal patterns are compared with the standard ECG and PPG patterns. The dynamic time wrapping method uses the distance cost as a similarity score between a single period of the ECG/PPG signal and the generated period Orphanidou et al. (2014). The package also implements other SQIs which evaluate the power energy on the

该用法围绕数据和规则模块中的三个类构建。

- 信号SQI对象具有原始信号、SQI表和基于规则的分类设置的属性。对象通过阅读波形初始化，并在每一步更新。
- 规则对象是为每个SQI构建的，具有用户定义的阈值，用于将信号段分类为“接受”或“拒绝”。通过从JSON文件中阅读SQI字典来初始化许多规则对象。
- 规则对象是要在提取的SQI表上按顺序执行的一组规则对象。它是一种轻量级的，但有效的信号质量分类方法（在我们的实验中显示在3.5中）。rulerance对象也是从JSON文件初始化的。资源模块中提供了这些JSON配置文件的模板以及我们推荐的阈值。

预处理和公共特征这两个模块共享支持功能，以便为SQI提取（如滤波、修整或R峰检测）准备信号。最后，我们提供了一个基于Web的GUI，它可以很容易地用来构造规则和规则集，并在输入SQI表上执行它们。结合用于SQI提取的Pipeline模块中提供的管道，该应用程序模块允许用户快速获得质量指标并分离接受和拒绝的信号段。

2.3 信号质量指标为了区分可用和不可用的信号段，在这项工作中实现的SQI已经被选择为允许灵活使用，适合于预处理前后的信号分类。因此，第一步是通过信号持续时间或通过节拍进行信号分段，即，每个段相当于一个周期（PPG）或QRS波群（ECG）。如表2.3.1所示，该封装具有七个峰值检测器。可用的SQI分为四个类别，对应于四个模块，如稍后所述。

2.3.1 峰值检测器使用vital_sqi包处理数据时，共有七种不同的峰值检测器可供选择。表中简要概述如下：

鼓励用户在处理特别嘈杂的数据集时使用不同的峰值检测器进行实验。每个检测器的性能受数据集的先前预处理的类型和程度的影响。

算法 ID	峰值检测器 name	输入 参数	源
1	自适应阈值		Shin等人（2009年）
2	计数原点		舍费尔和 03 The Dog（2008）
3	聚类		
4	斜率和		Zong等人（2003年）
5	均线		Elgendi等人 (2013)
6	默认SciPy		维尔塔宁等人 (2020)
7	比劳尔算法		03 The Dog（2009）

2.3.2 统计SQI统计SQI分析段内的信号趋势，提供潜在概率分布的特征。实施的SQI建立在Elgendi（2016）之前的工作基础上。在过去的十年中，已经对利用统计SQI来确定PPG信号质量进行了大量研究，在区分可接受和不适合的信号段时显示出有希望的性能（Selvaraj 等人，2011；Krishnan 等人，2010；Elgendi，2016）。将统计SQI与此包中提供的其他SQI相结合，进一步提高了它们的引用性能，并允许研究人员微调其信号质量选择标准。有关可用的基于语法的SQI的完整列表，请参阅表1。

2.3.3 基于心率变异性和平均RR间期的SQI

在其他操作模式中，检查识别信号内的连续R波（对于ECG）或收缩峰（PPG）的准确度。基于RR间隔的SQI在检测RR峰值的不同方法之间获得共识。

除了纯粹的SQI计算，HRV指数是从RR信号计算的，这可以允许关于心脏和神经系统功能和控制的推断。使用该软件包，HRV是由一系列的过程：过滤，rescribe，峰值检测，去除假峰，并提取特征。这些步骤是必要的，因为信号质量差可能导致R波标记不准确和HRV指标不准确。具体地，频域和时域中的HRV特征在正常和患病患者之间是可区分的，并且在人类中是不可观察的，这指的是差的质量。

2.3.4 基于波形的SQI在计算这些指数时，将信号模式与标准ECG和PPG模式进行比较。动态时间包络方法使用距离成本作为ECG / PPG信号的单个周期与所生成的周期之间的相似性分数。Orphanidou 等人（2014）。该软件包还实现了其他SQI，用于评估

bands of the QRS complex [Marco et al. \(2012\)](#). Other SQIs mentioned in this section evaluate the peak-to-nadir amplitude in the ECG and the systolic-diastolic amplitude ratio in the PPG.

2.4 Decision ruleset

As vital signals can be collected from different devices with different modes of operation, a winner-take-it-all method is unfeasible in making signal quality decisions. In practice, the statistical SQIs are appropriate to the longer segments of the signal but highly sensitive to noise and artifacts, which makes selection of the optimal length important. On the other hand, morphology-based SQIs are useful for observing the shorter segments, but the results can be misleading if the underlying waveform is not well-segmented. Our package is advantageous in that it allows flexibility in creating a ruleset by combining various SQIs scores and, thus, can be adapted for multiple scenarios. User-defined rules are set as a chain of SQIs scores using a simple-to-use graphical interface.

3 Recommended workflow and experiments

In this section, we present a step-by-step demonstration of the package. This workflow is already designed in the “high-level” module. Users can either get the SQIs list immediately by importing this module or design their own flow using the other modules. The vital-sqi package is composed of the following steps: preprocessing, segmentation, sqi computation,

and rule definition. Both ECG and PPG data are used for this demonstration.

3.1 Preprocessing

The main objective of this step is to transform the raw data to match with a standard template of ECG/PPG. First, the signal is checked to remove any missing data or invalid data when reading a given file format. Noise removal is performed by applying the bandpass filter with the appropriate methodology. The Butterworth is the default approach as it provides a good baseline performance and significantly enhances the complex. [Figure 2](#) shows the output using the bandpass method from the package on both ECG and PPG.

In addition to the bandpass filter function, the preprocessing module also implements other techniques to sharpen and expose the signal further such as tapering and resampling. This recommended workflow only filters the signal and removes the missing data. Other preprocessing functions will only be employed later in the SQI computation steps. At the end of the preprocessing process, the package marks chunks of certainly invalid signals. The package considers any available values, unchanged sequences, and zero-unit values as invalid signals. Only chunks of valid signals are used for computation of SQI scores.

3.2 Segmentation

Once clean data are obtained, the signal is split into chunks of shorter intervals. Depending on user preference, the segmentation length can be defined in minutes or seconds. Based on our sample

TABLE 1 List of well-known SQIs available in the `vital_sqi` Python package.

SQI name	Type	Signal	Equation or brief description	Per segment	Per beat	Introduced as SQI in
Perfusion	Stats	PPG	$P_{SQI} = \frac{(y_{\max} - y_{\min})}{ x } \times 100$	Y	N	
Kurtosis	Stats	PPG	$K_{SQI} = \frac{1}{N} \sum_{i=1}^N \left[\frac{x_i - \bar{x}}{\sigma} \right]^4$	Y	Y	Selvaraj et al. (2011)
Skewness	Stats	PPG	$S_{SQI} = \frac{1}{N} \sum_{i=1}^N \left[\frac{x_i - \bar{x}}{\sigma} \right]^3$	Y	Y	Krishnan et al. (2010)
Entropy	Stats	PPG	$E_{SQI} = -\sum_{i=1}^N x(n)^2 \log_e(x(n)^2)$	Y	Y	Selvaraj et al. (2011)
SNR	Stats	PPG and ECG	$N_{SQI} = \frac{\sigma_{signal}^2}{\sigma_{noise}^2}$	Y	N	Elgendi (2016)
Relative power	Stats	PPG and ECG	$R_{SQI} = \frac{\sum_{j=1}^{2.25} PSD}{\sum_{j=0}^8 PSD}$	Y	N	Elgendi (2016)
Mean crossing	Stats	PPG	Number of mean crossings within the signal segment	Y	N	
Zero crossing	Stats	PPG and ECG	Number of zero crossings within the signal segment	Y	N	Elgendi (2016)
MSQ	Morph	PPG	Degree of agreement between two distinct peak detector algorithms	Y	N	Elgendi (2016)
Correlogram	Stats	PPG and ECG	Location and prominence of peaks of the signal segment correlogram	Y	N	Pradhan et al. (2017)
Dynamic time warping	Morph	PPG and ECG	Template matching of a single period with a mathematically described ideal period	N	Y	Li and Clifford (2012)

Marco et al. (2012) .本节中提到的其他SQI评价ECG中的峰底振幅和PPG中的收缩-舒张振幅比。

2.4 决策规则由于可以从具有不同操作模式的不同设备收集生命信号，因此赢家通吃的方法在做出信号质量决策时是不可行的。在实践中，统计SQI适用于信号的较长段，但对噪声和伪影高度敏感，这使得选择最佳长度很重要。另一方面，基于形态学的SQI对于观察较短的段是有用的，但是如果底层波形没有很好地分段，则结果可能是误导性的。我们的软件包是有利的，因为它允许灵活地创建一个规则，通过结合各种SQIs 分数，因此，可以适应多种情况。使用简单易用的图形界面，用户定义的规则被设置为SQI分数链。

规则定义。ECG和PPG数据均用于此演示。

3.1 预处理此步骤的主要目的是转换原始数据以与ECG / PPG的标准模板匹配。首先，在阅读给定文件格式时，检查信号以移除任何丢失的数据或无效数据。噪声去除是通过应用带通滤波器与适当的方法。巴特沃思是默认方法，因为它提供了良好的基线性能，并显著增强了复杂性。图2显示了使用带通方法从ECG 和PPG上的封装输出。

除了带通滤波器功能之外，预处理模块还实现了其他技术来进一步锐化和暴露信号，例如锥形化和重新扩展。此推荐的工作流仅过滤信号并删除丢失的数据。其他预处理函数将仅在稍后的SQI计算步骤中使用。在预处理过程结束时，包标记了肯定无效的信号块。该包将任何可用值、未更改的序列和零单位值视为无效信号。只有有效信号块用于计算SQI分数。

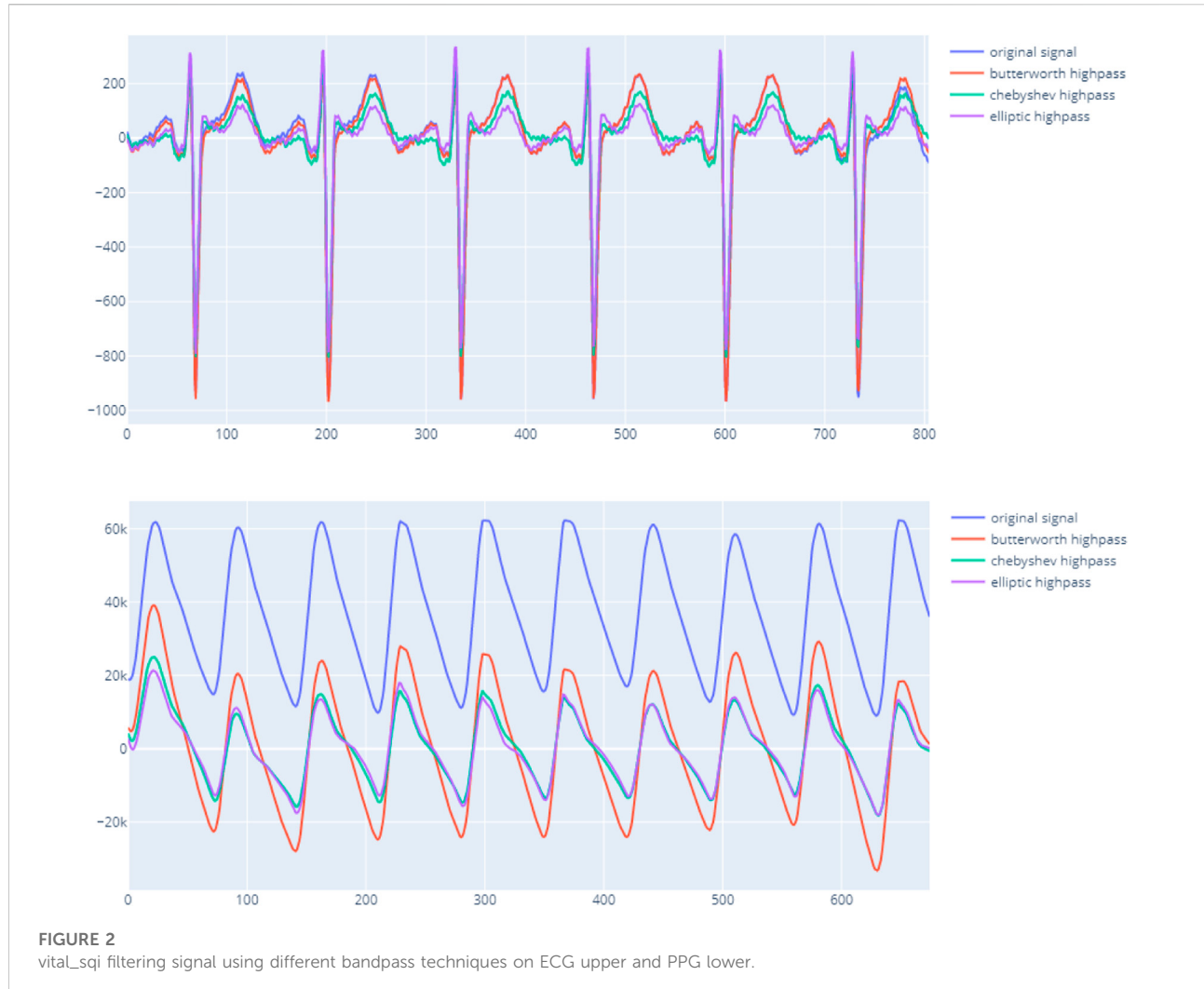
3推荐的工作流程和实验

在本节中，我们将逐步演示该软件包。此工作流程已在“高级”模块中设计。用户可以通过导入此模块立即获得SQI列表，也可以使用其他模块设计自己的流。vital-sqi包由以下步骤组成：预处理，分割，sqi计算

3.2 分割一旦获得干净的数据，信号被分成较短间隔的块。根据用户的偏好，分段长度可以以分钟或秒为单位定义。根据我们的样本

表1 vital_sqi Python包中可用的知名SQI列表。

SQI名称	Type	信号	方程或 简要说明	Per 段	Per beat	介绍为 SQI输入
灌注	统计数据	PPG	P × 100	Y	N	
峰度	统计数据	PPG	K Σ[]	Y	Y	Selvaraj等人 (2011年)
偏度	统计数据	PPG	S Σ[]	Y	Y	Krishnan等人 (2010)
熵	统计数据	PPG	E -Σx (n) log (x (n))	Y	Y	Selvaraj等人 (2011年)
SNR	统计数据	PPG 和ECG	N	Y	N	02 The Fall (2016)
相对功率	统计数据	PPG 和ECG	R Σ	Y	N	02 The Fall (2016)
平均交叉	统计数据	PPG	信号段内的平均交叉数	Y	N	
零交叉	统计数据	PPG 和ECG	信号段内的过零点数	Y	N	02 The Fall (2016)
MSQ	变形	PPG	两种不同峰值检测器算法之间的一致程度	Y	N	02 The Fall (2016)
相关图	统计数据	PPG 和ECG	信号段相关图峰值的位置和突出度	Y	N	Pradhan等人 (2017)
动态时间 翘曲	变形	PPG 和ECG	单周期与数学描述的理想周期的模板匹配	N	Y	李和克利福德 (2012)



data, we recommend a segment length of 30 s as long enough to compute HRV features while maintaining the SQI scores less vulnerable to noise and artefacts compared to long segments. In addition, using shorter signal chunks improves the accuracy of the subsequent peak detection algorithms.

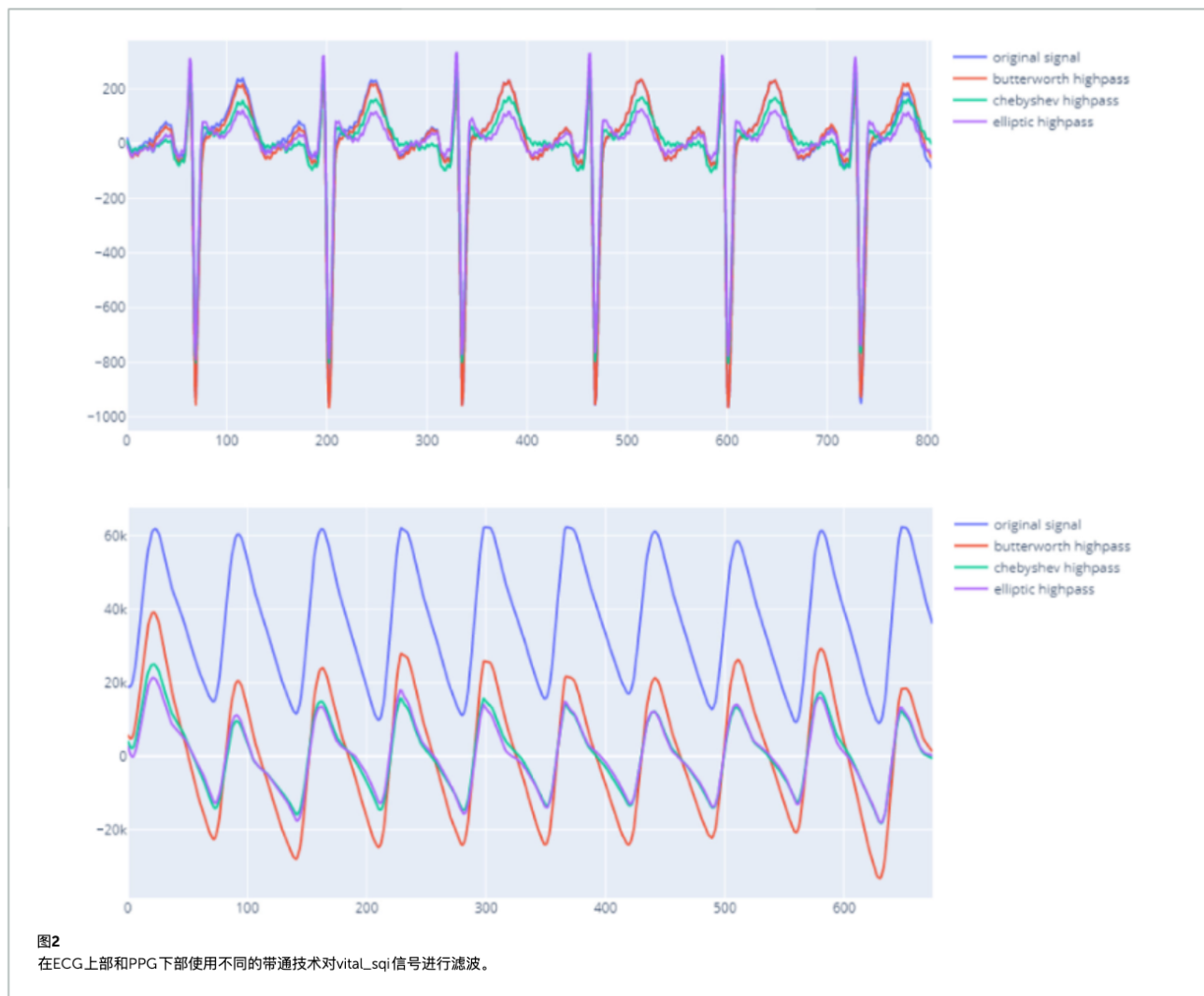
From this point, users can manipulate the signal further with preprocessing methods such as resampling to enhance the single waveforms. Alternatively, peak detection can be performed in advance to get the local minima, which maps to the troughs of the signal and can serve as splitting points. However, it is not recommended at this stage because of the heavy computational load and ineffectiveness when processing long data sequences. Furthermore, peak detection will be employed later for SQI computation.

3.3 SQI computation

As explained in [Section 2](#), the SQI can be computed either using the entire segment or single beats. This step produces a matrix of SQI

scores of each segment by applying all possible SQI computations. The SQI module implements all of the reviewed methods and categorizes them into hrv_sqi, standard_sqi, and rpeaks_sqi submodules. Since computing all of the available SQIs is time-consuming, users can select a smaller subset of indices. However, we strongly encourage using at least two SQI techniques from each of these subpackages and at least two that use single beats to preserve the accuracy.

In case of a single-beat algorithm, the mean and standard deviation of all beats within the segment are calculated to contribute to the matrix scores. In detail, the peak detection methods on ECG or PPG are applied in each chunk to extract beats. The extracted beats are transformed by resampling, tapering, and smoothing window techniques to enhance and unify the beat baseline. [Figure 3](#) indicates the importance of enhancing beats before computing SQIs. Particularly, the HRV SQIs are highly sensitive to the appearance of any abnormal spikes. By enhancing the signal, critical points are easier to detect and, hence, increase the accuracy. In addition, the zero crossing rate, mean crossing rate, and dynamic template indices also



数据，我们建议30 s的段长度足够长以计算HRV特征，同时保持SQI分数与长段相比不易受噪声和伪影的影响。此外，使用较短的信号块提高了后续峰值检测算法的准确性。

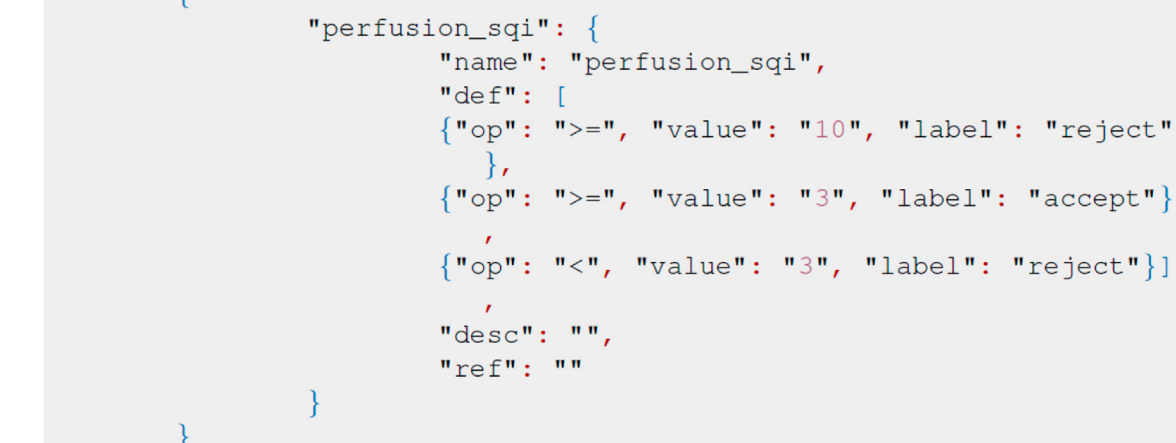
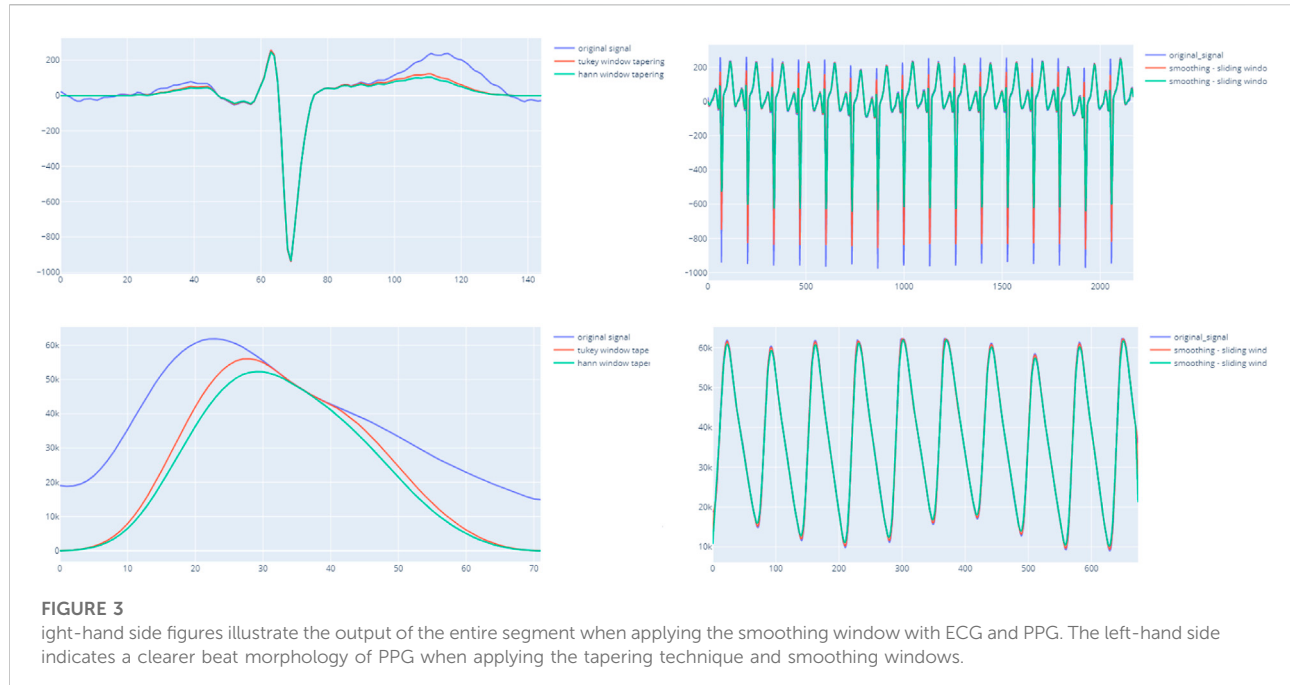
从这一点来看，用户可以通过预处理方法（如重采样）进一步处理信号，以增强单个波形。或者，可以提前执行峰值检测以获得局部最小值，该局部最小值映射到信号的波谷并且可以用作分裂点。但是，由于在处理长数据序列时计算量大且效率低，因此不建议在此阶段使用。此外，峰值检测稍后将用于SQI计算。

此步骤通过应用所有可能的SQI计算来产生每个片段的SQI分数矩阵。SQI模块实现了所有检查过的方法，并将它们分类为hrv_sqi、standard_sqi和rpeaks_sqi子模块。由于计算所有可用的SQI非常耗时，因此用户可以选择较小的索引子集。但是，我们强烈建议使用至少两种来自每个子包的SQI技术，以及至少两种使用单节拍的SQI技术来保持准确性。

在单次搏动算法的情况下，计算段内所有搏动的平均值和标准差以贡献于矩阵分数。详细地，在每个块中应用ECG或PPG上的峰值检测方法以提取搏动。提取的心搏通过恢复、逐渐变细和平滑窗口技术进行变换，以增强和统一心搏基线。图3显示了在计算SQI之前增强节拍的重要性。特别地，HRV SQI对任何异常尖峰的出现高度敏感。通过增强信号，临界点更容易检测，从而提高准确性。此外，过零率、平均过零率和动态模板指数也

3.3 SQI计算

如第2节所述，SQI可以使用整个段或单个节拍来计算

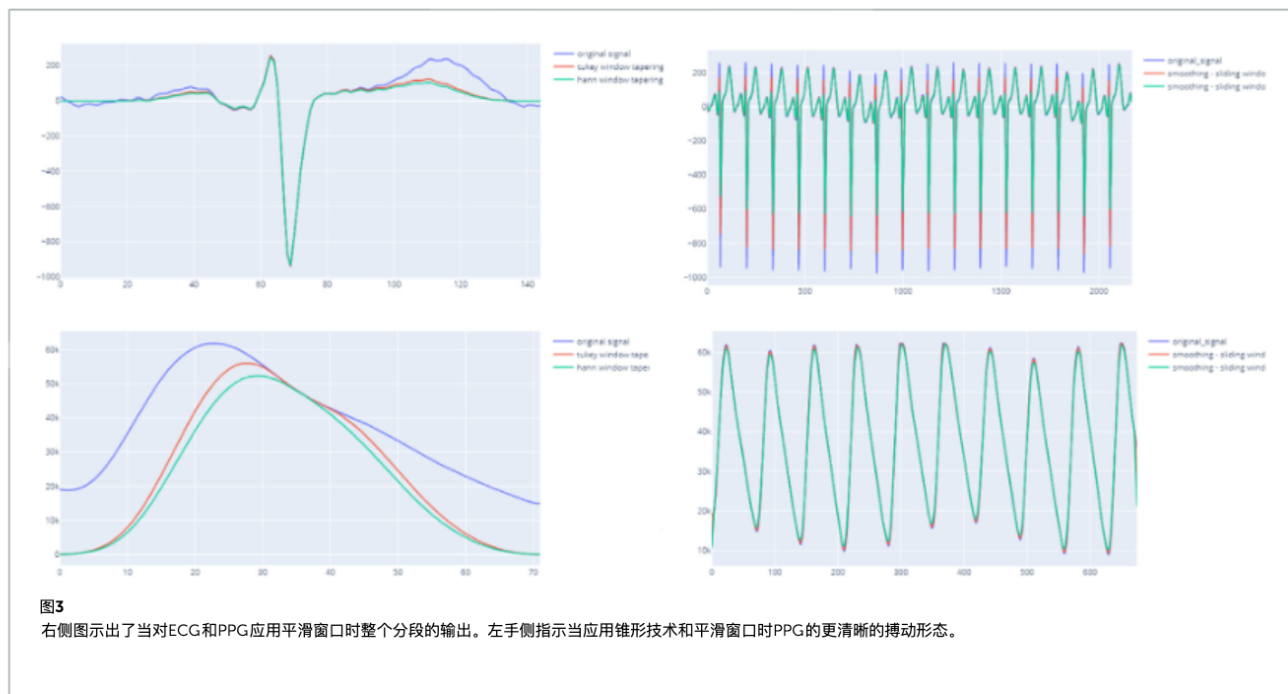


require unification of the baseline. The computed matrix is then input to the final decision ruleset.

3.4 Rule definition

The package defines the ruleset in the JSON format with the key node being the same as the SQI method. Each child node describes the acceptance threshold, score, and relevant

decision. The sample JSON format in Figure 4 represents the rule definition using the kurtosis, skewness, and entropy scores as the decision node. The order of selected SQIs can be modified through the JSON file accordingly. In this package, we also provide the recommended threshold for specific SQI scores. The recommended JSON is located in the test_data module, and the values given are derived from our real dataset. When applying numerous SQI scores, modifying JSON can be time-consuming and impractical,



需要统一基线。然后将计算出的矩阵输入到最终的决策规则中。

3.4 规则定义该包以JSON 格式定义规则，关键节点与SQI方法相同。每个子节点描述接受阈值、分数

相关决定。图4中的示例JSON格式表示使用峰度、偏度和熵分数作为决策节点的规则定义。可以通过JSON文件相应地修改所选SQI的顺序。在这个包中，我们还提供了特定SQI分数的推荐阈值。推荐的JSON位于test_data 模块中，给出的值来自我们的真实的数据集。当应用多个SQI分数时，修改JSON可能是耗时且不切实际的，

and therefore, we have developed a GUI for ruleset modifications.

The GUI is launched as a local web-based application using the DASH framework and Plotly for visualization. The interface is designed using three main dashboards. The home page is used to read the input SQI matrix and the saved ruleset. The uploaded matrix is displayed on the first dashboard, while the loaded ruleset is presented on the second.

Based on user preference, some or all SQI scores can be selected by toggling the rule name button. Each SQI score can have multiple thresholds, different orders and combinations of rules. The final decision will be verified in the third dashboard that will also output the final decision.

3.5 Experiment

The experiment aims to demonstrate how the package could be used to label the signal. With an in-house curated dataset, we derived suggestive thresholds for the included SQIs and evaluated the performance of simple rules in signal quality classification.

3.5.1 Dataset

The learning dataset contains the PPG waveforms collected from patients with tetanus treated in the Intensive care unit, lying in a supine position. The device used was the SmartCare oximeter. The study was approved by the ethics committee of the Hospital of Tropical Diseases, Ho Chi Minh City, Vietnam. From 70 long recordings for an average 20 h, we randomly selected 383 30-s segments. These were double-annotated by doctors as accept or reject based on visual appearance of the waveforms. In the training set, we have a list of criteria to determine the quality of the data segment. The data are annotated by a tool as demonstrated in [Figure 5](#). In this tool, besides the percentage of recognizable peaks, the tool also requires the doctor to mark if the amplitude, width, and trend are abnormal. The annotation process was composed of two rounds. Any uncertain segment in the first round was reserved for the second round. After the first round, 72% of the segments were labeled. In the second round, the opposite decision was made in less than 10% of labeled segments. Most of the changed segments occurred in the initial segments, when the doctor was unfamiliar with the dataset. Although the multi-criterion tool assured high quality annotation, it is time-consuming and also annotates unused factors.

Consequently, from the list of well-annotated segments, the waveform-based criteria were simplified to possessing visible systolic and diastolic peaks and the presence of artifacts as presented in [Figure 6](#). The resultant dataset included 273 accepted (A) and 114 rejected segments (NG). The rejected segments were further divided into two groups based on the percentage of cycles with unrecognizable peaks: more than 50% (NG1, 47 segments) and less than 50% (NG2, 67 segments).

The same simplified format is applied for the test dataset. This test dataset was composed of 900 accepted segments and 279 rejected segments (210 in NG1 and 69 in NG2).

This training data were then used to determine the thresholds for each SQI. The threshold is defined by a greedy search process, in which the step size is 0.1 quantile unit. The experiments followed the previously described pipeline to obtain the list of relevant SQI scores. Although users can decide the SQIs based on their experience, this package introduces an intuitive yet efficient approach to derive the thresholds. Specifically, the distributions are examined to mark the potential SQI and the appropriate threshold.

3.5.2 Settings

We conducted two experiments, as follows:

- 1) SQI threshold derivation: For each SQI implemented in the package, we use two methods to determine a threshold that differentiates accept and reject segments. First, the threshold is set as the 95th percentile of the accept histograms. Second, the threshold is determined by a brute force search (step is 0.05 on the quantile) for the most discriminative of the accept and reject segments.
- 2) Rule building: We searched for the combinations of SQIs that best differentiate the accept and reject segments from the SQIs with the best performances identified earlier; our aim being to show that the combination SQIs (even only two), in a simple rule-based decision approach, result in reasonably good quality assignment.

3.5.3 Results

Using the recommendation in the aforementioned pipeline, we conducted the experiments using a single SQI and a combination of two SQIs. A greedy search was used to verify the performance of all combinations. The final result of the best 10 combinations is illustrated in the table.

As presented in [Figure 7](#), a list of SQIs which compute both per beat and per segment are selected. Looking further into the nominated SQIs, the interpretation is explained as follows:

- 1) Entropy: This indicates the probability of the appearance of the signal at certain levels. The normal signal of the heart rate is distributed in a normal distribution. In case of an invalid signal, the probability of the appearance of the signal at a certain level is adjusted. Regions that appear rarely can be observed, and it reduces the probability of the normal range. Hence, the information entropy is discriminatory.
- 2) Mean_nni: This score indicates the mean value of the normal to normal interval (i.e., successive beats). The nni is computed from specific ECG or PPG data. Hence, the result will be extremely vulnerable to any noise and artifacts. In general, the distribution is a normal distribution, and when there is noise, the distribution becomes uniform.

因此，我们开发了一个用于规则修改的GUI。

GUI作为基于Web的本地应用程序启动，使用DASH框架和Plotly进行可视化。该界面使用三个主要仪表板设计。主页用于读取输入SQI矩阵和保存的规则。上传的矩阵显示在第一个仪表板上，而加载的规则显示在第二个仪表板上。

根据用户偏好，可以通过切换规则名称按钮来选择部分或全部SQI分数。每个SQI分数可以有多个阈值，不同的顺序和规则组合。最终决定将在第三个仪表板中进行验证，该仪表板也将输出最终决定。

同样的简化格式也适用于测试数据集。该测试数据集由900个接受的片段和279个拒绝的片段组成（NG1中210个，NG2中69个）。

然后使用该训练数据来确定每个SQI的阈值。阈值由贪婪搜索过程定义，其中步长为0.1分位数单位。实验遵循先前描述的流水线以获得相关SQI分数的列表。虽然用户可以根据他们的经验决定SQI，但这个包引入了一种直观而有效的方法来获得阈值。具体而言，检查分布以标记潜在的SQI和适当的阈值。

3.5.2 设置

我们进行了两个实验，如下所示：

3.5 实验该实验旨在演示如何使用该软件包标记信号。通过内部策划的数据集，我们为所包含的SQI导出了建议性阈值，并评估了信号质量分类中简单规则的性能。

3.5.1 数据集学习数据集包含从重症监护室中接受治疗的破伤风患者收集的PPG波形，患者以仰卧位躺下。所用器械为SmartCare血氧计。该研究得到了越南胡志明市热带病医院伦理委员会的批准。从平均20小时的70个长录音中，我们随机选择了383个30秒的片段。医生根据波形的视觉外观对这些进行双重注释，作为接受或拒绝。在训练集中，我们有一系列标准来确定数据段的质量。如图5所示，通过工具注释数据。在该工具中，除了可识别峰的百分比之外，该工具还要求医生标记振幅、宽度和趋势是否异常。注释过程分为两轮。第一轮中任何不确定的部分都保留到第二轮。在第一轮之后，72%的片段被标记。在第二轮中，在不到10%的标记片段中做出了相反的决定。大多数变化的片段发生在初始片段中，当时医生不熟悉数据集。虽然多标准工具保证了高质量的注释，但它很耗时，而且还会注释未使用的因子。

因此，从注释良好的节段列表中，基于波形的标准被简化为具有可见的收缩和舒张峰值以及伪影的存在，如图6所示。所得数据集包括273个接受的片段（A）和114个拒绝的片段（NG）。根据无法识别峰的循环百分比，将拒绝的节段进一步分为两组：大于50%（NG 1，47个节段）和小于50%（NG 2，67个节段）。

1)SQI阈值推导：对于包中实现的每个SQI，我们使用两种方法来确定区分接受段和拒绝段的阈值。首先，将阈值设置为接受直方图的第95个百分位数。其次，通过强力搜索（步长为0.05分位数）确定接受和拒绝段中最具鉴别力的阈值。2)规则建设：我们搜索的SQIs的组合，最好区分接受和拒绝段与SQIs的最佳性能较早确定；我们的目的是要表明，组合SQIs（即使只有两个），在一个简单的基于规则的决策方法，导致合理良好的质量分配。

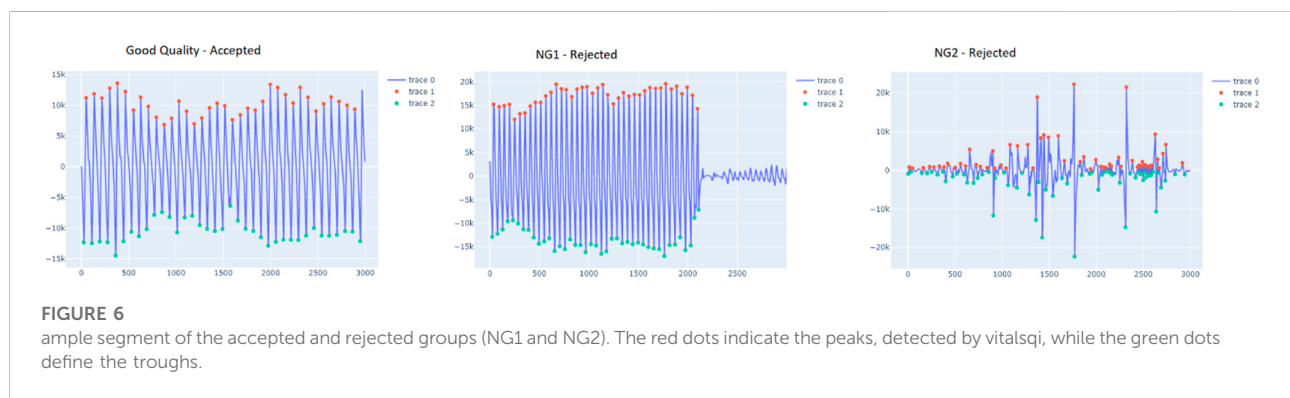
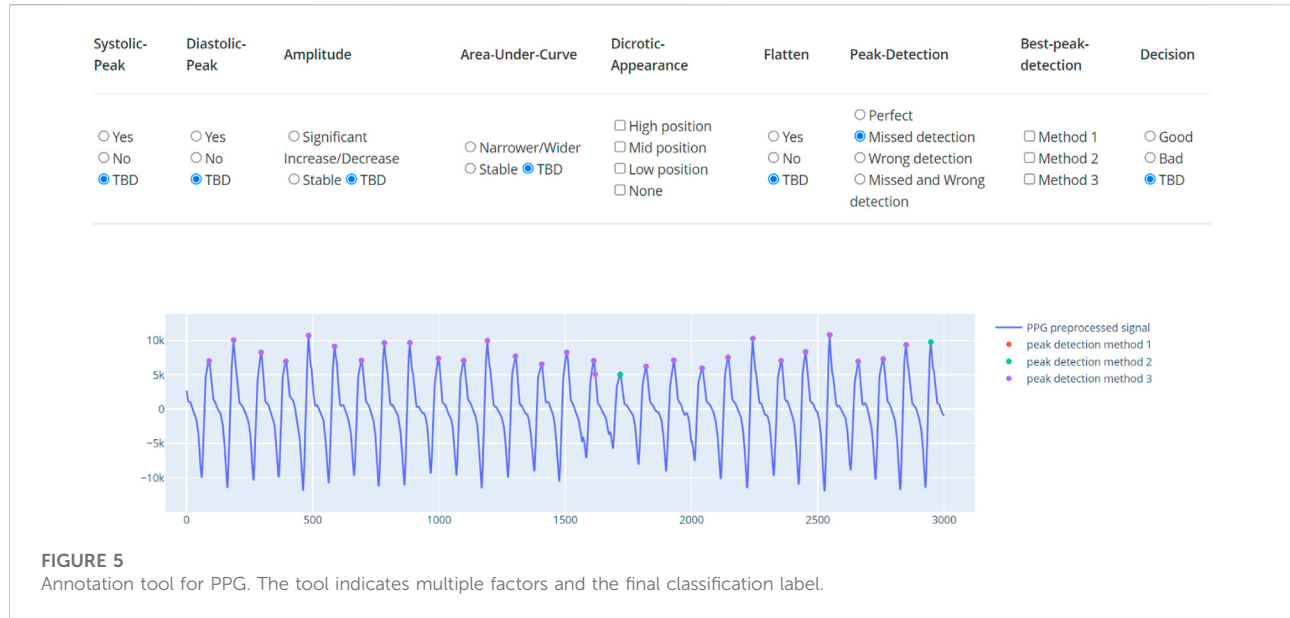
3.5.3 结果使用上述管道中的建议，我们使用单个SQI和两个SQI的组合进行实验。使用贪婪搜索来验证所有组合的性能。最佳10个组合的最终结果如表所示。

如图7所示，选择了计算每个心跳和每个分段的SQI列表。进一步审视提名SQI，解释如下：

1)熵：这表明信号在某些水平上出现的概率。心率的正态信号以正态分布进行分布。在无效信号的情况下，调整信号出现在特定水平的概率。很少出现的区域可以被观察到，并且它降低了正常范围的概率。

因此，信息熵是有区别的。

2)Mean_nni：该分数指示正常到正常间隔的平均值（即，连续节拍）。根据特定ECG或PPG数据计算nni。因此，结果将非常容易受到任何噪声和伪影的影响。一般来说，该分布是正态分布，当存在噪声时，该分布变得均匀。

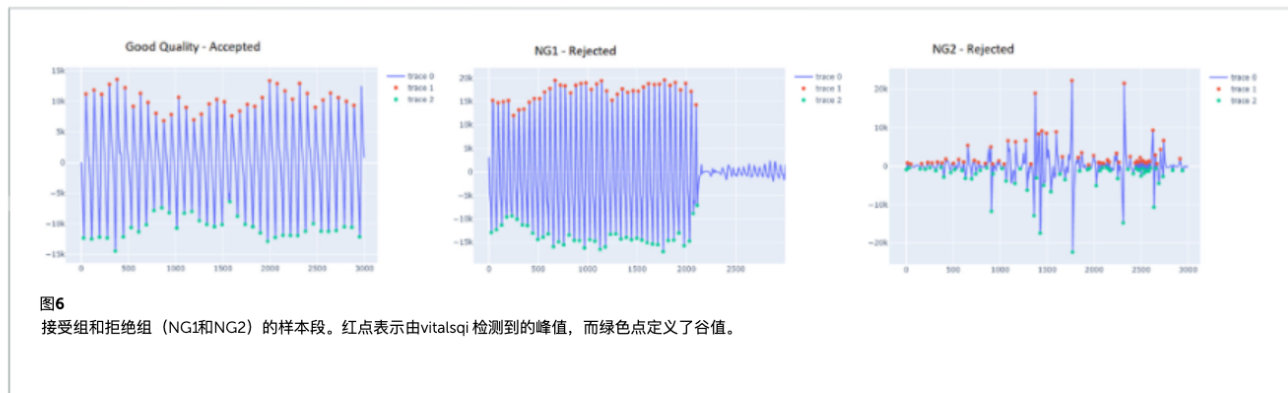
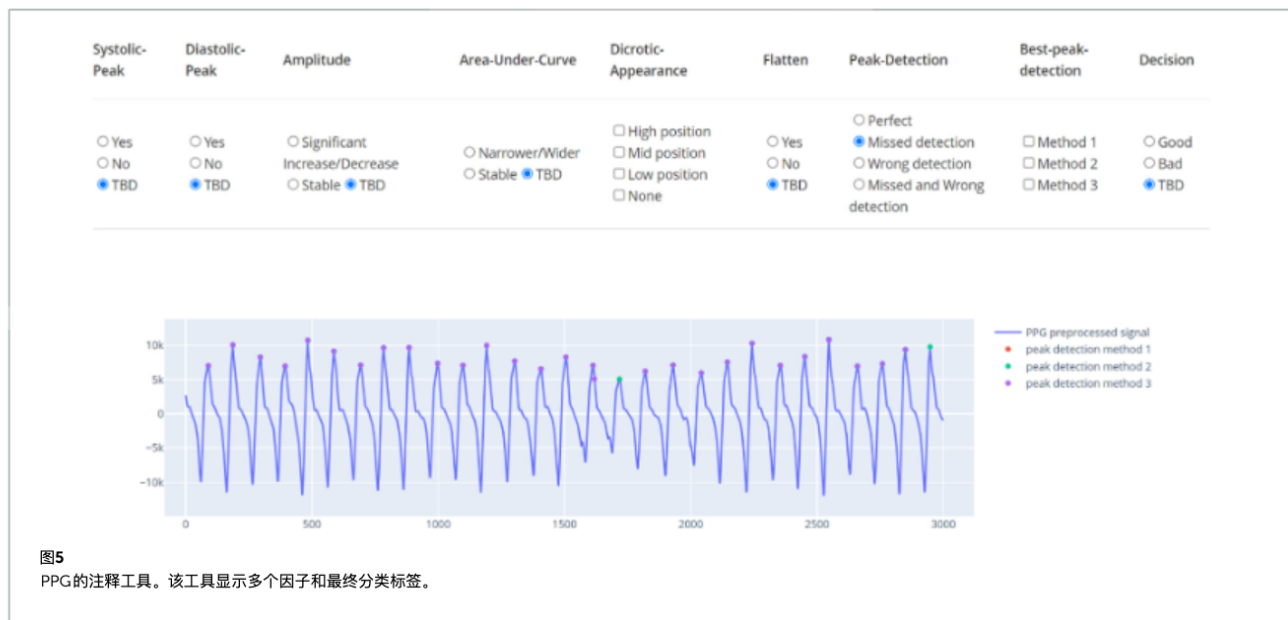


- 3) MSQ: This SQI computes the consistency of the peak detection algorithm. The signal is shifted n-seconds forward and performs the same peak detection. Assuming the signal is of good quality, the location of the n-second later peak does not vary significantly. However, noise will cause multiple spikes, which potentially result in misreading of the peak and hence inconsistency.
- 4) Pnn_50: This shows the ratio between NN50 and the total number of heartbeat intervals. NN50 is the number of times successive heartbeat intervals exceed 50 ms, and is believed to be associated with parasympathetic nervous system activity. A bad quality signal leads to increase of the score.
- 5) SDNN: Among many HRV features, SDNN is the most representative. The score represents the standard deviation of beat-to-beat intervals. Some medical sources use this as the main indicator of HRV, and it is defined that the normal range of HRV is 20–60. As the signal is heavily damaged by

the artifact, the SDNN results in greater scores that exceed the normal range.

Following the greedy search process, the results were as follows. According to the distribution, the SQI score differs significantly between the per-beat and per-segment calculation. In terms of the rejection rate, the performance of SQIs per segment is more accurate. Since per-beat analysis mainly depends on beat segmentation, the longer the sequence is, the less accurate the SQI computes. By experimenting with different time lengths, the 30-s segment was observed to be the most appropriate duration. Within this interval, the sequence is long enough to derive meaningful clinical features such as HRV and is also efficient to split by beat.

In summary, using a single SQI as in Table 2, the best 10 combinations using two SQIs compute in per segment, and the rest computes in HRV (which refers to both per beat and per segment). The SQIs are ranked by the AUC rather as the package aims to eliminate as many invalid signals as possible, while retaining a



3)MSQ：此SQI计算峰值检测算法的一致性。信号向前移动n秒，并执行相同的峰值检测。假设信号质量良好，则n秒后峰值的位置不会显著变化。然而，噪声将导致多个尖峰，这可能导致峰的误读，从而导致不一致。4)Pnn_50：显示NN 50与心跳间期总数的比值。NN 50是连续心跳间隔超过50 ms的次数，被认为与副交感神经系统活动有关。质量差的信号导致分数增加。5)SDNN：在众多的HRV特征中，SDNN最具代表性。该分数表示心跳间隔的标准差。一些医学资料将此作为HRV的主要指标，并定义HRV的正常范围为20-60。由于信号被严重破坏，

伪影，SDNN 导致超过正常范围的更大分数。

经过贪婪搜索，结果如下。

根据分布，SQI分数在每心跳和每段计算之间显著不同。在拒绝率方面，每个段的SQI的性能更准确。由于逐拍分析主要依赖于拍分割，因此序列越长，SQI计算的准确度就越低。通过对不同时间长度的试验，观察到30秒段是最合适的持续时间。在该间隔内，序列足够长以导出有意义的临床特征，例如HRV，并且还可以有效地按心跳进行分割。

总之，使用如表2中的单个SQI，使用两个SQI的最佳10个组合在每个分段中计算，并且其余组合在HRV中计算（其指的是每个搏动和每个分段两者）。SQI是按AUC排序的，因为软件包旨在消除尽可能多的无效信号，同时保留

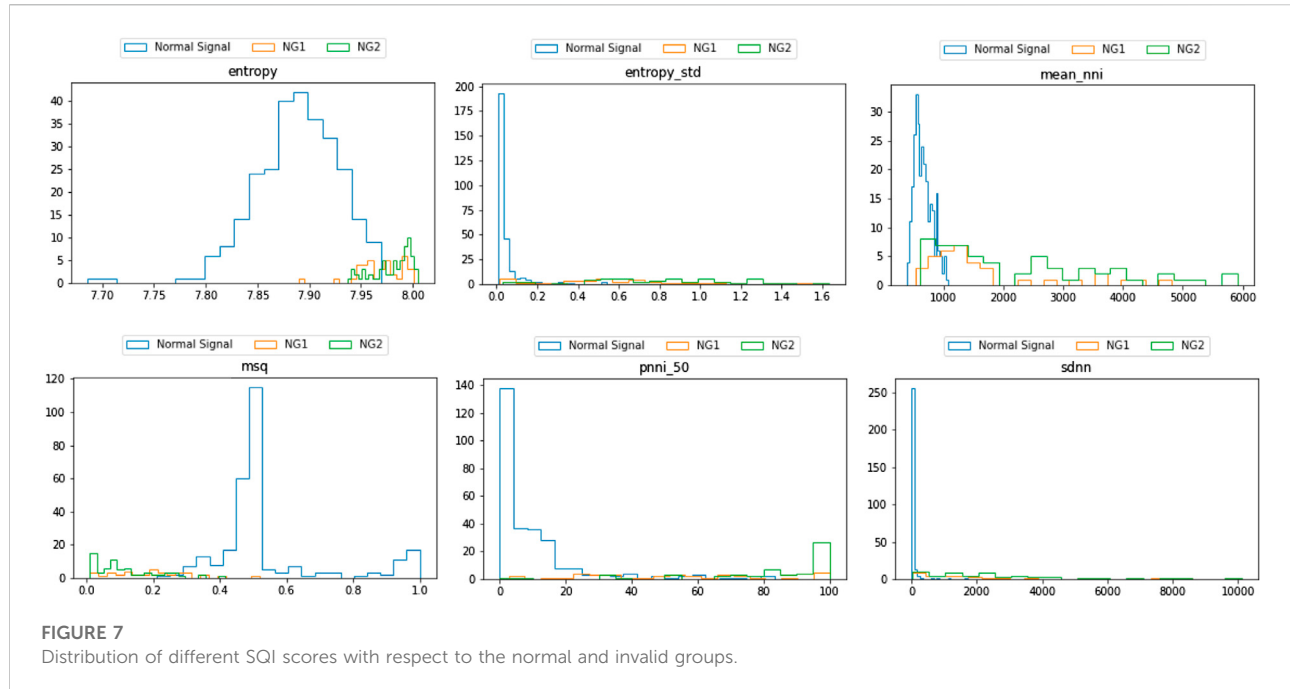


TABLE 2 Performance of each sqi in classifying a good-quality segment.

Rule	Good accuracy	R1 accuracy	R2 accuracy	Accuracy	Brier	Roc	Fbeta
CVSD	0.9067	0.7095	0.942	0.8024	0.1264	0.8368	0.8761
SDNN	0.9067	0.6667	0.8986	0.7973	0.1366	0.8153	0.8644
RMSSD	0.9078	0.6571	0.8986	0.7981	0.1374	0.81 23	0.8631
SDSD	0.9156	0.6429	0.8696	0.8007	0.1357	0.8072	0.8632
Entropy STD	0.9356	0.619	0.8406	0.8126	0.1264	0.8047	0.8699
Power	0.8889	0.6571	0.8841	0.782	0.1527	0.8011	0.8505
CVNNI	0.9144	0.6333	0.8116	0.793	0.1416	0.7959	0.8566
LF	0.88	0.6571	0.8261	0.7684	0.1629	0.7895	0.8411
HF	0.8489	0.6619	0.9275	0.7566	0.1798	0.7882	0.8314
Heart rate STD	0.9189	0.5286	0.8696	0.8032	0.1535	0.7659	0.8415

large amount of good-quality signals for later analysis. Generally, all SQIs are effective at identifying the severely distorted signals (R2 group) showing accuracy of above 80%, with most of them (SVSD, SDNN, RMSSD, and SDSD) above 88%. However, the SQIs differ when validating the quality of the R1 group. Most of the SQIs performed with only 60–65% accuracy. Only one SQI (CVSD) reached 70%, while the worst performing SQI (heart rate standard deviation) has only 50% accuracy. Importantly, however, in terms of retaining good-quality signals, all SQIs performed well and retain approximately 90% of valid signals.

In case of combined SQIs described in Table 3, the rejected cases were significantly higher. The 10 most successful combinations detected more than 90% of invalid signals in

the R2 group. With the R1 group, the rejected cases were increased, and all of the combinations obtained more than 70% accuracy, with one combination obtaining approximately 80% accuracy. However, this increased performance occurred at the expense of a decrease in accuracy in the good-quality group, where accuracy decreased from 89% to 83%. It is worth noting that the discard rate in the second invalid group was higher than that in the first invalid group, which reflects the fact that signals in the second group are much more distorted.

Examining the cases of misclassification, the waveform morphology of PPG signals did not fully match with the standard PPG since the diastolic peaks were indistinct. It is worth noting that these still have utility as the heart rate can

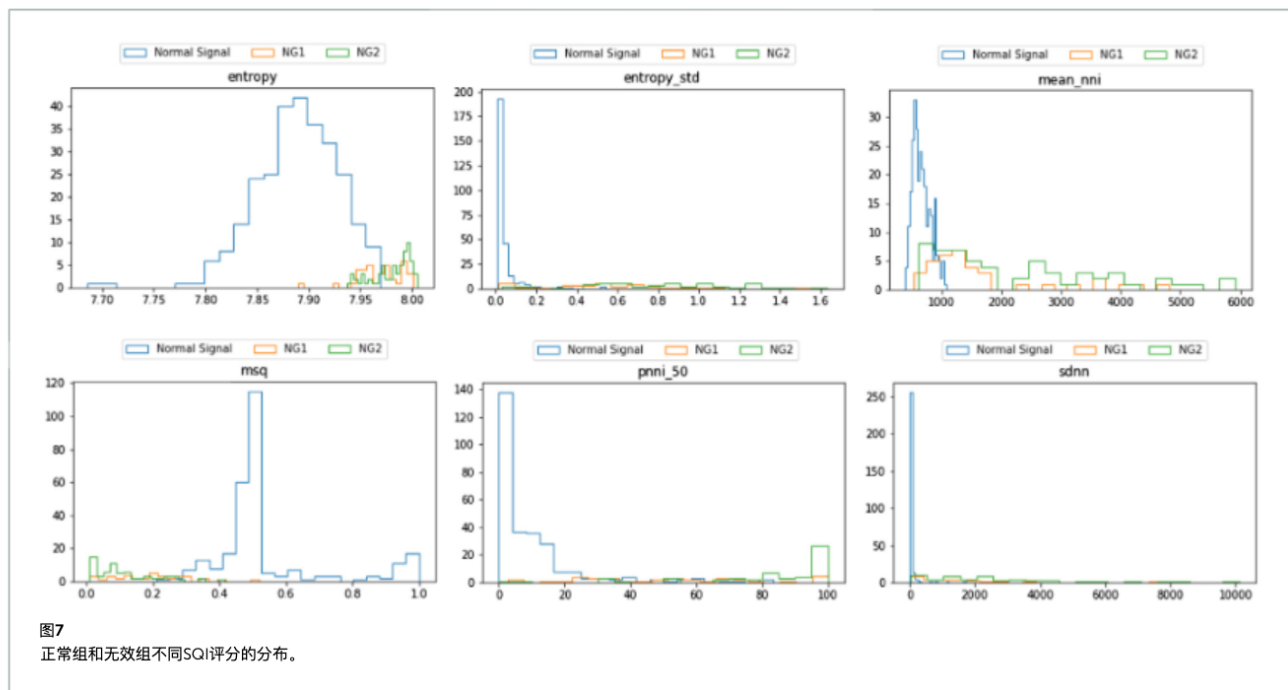


图7

正常组和无效组不同SQI评分的分布。

表2每个SQI在对高质量段进行分类时的性能。

Rule	良好的精度	R1准确度	R2准确度	精度	Brier	Roc	Fbeta
CVSD	0.9067	0.7095	0.942	0.8024	0.1264	0.8368	0.8761
SDNN	0.9067	0.6667	0.8986	0.7973	0.1366	0.8153	0.8644
RMSSD	0.9078	0.6571	0.8986	0.7981	0.1374	0.8123	0.8631
SDSD	0.9156	0.6429	0.8696	0.8007	0.1357	0.8072	0.8632
Entropy STD的使用	0.9356	0.619	0.8406	0.8126	0.1264	0.8047	0.8699
Power	0.8889	0.6571	0.8841	0.782	0.1527	0.8011	0.8505
CVNNI	0.9144	0.6333	0.8116	0.793	0.1416	0.7959	0.8566
LF	0.88	0.6571	0.8261	0.7684	0.1629	0.7895	0.8411
HF	0.8489	0.6619	0.9275	0.7566	0.1798	0.7882	0.8314
心率STD	0.9189	0.5286	0.8696	0.8032	0.1535	0.7659	0.8415

为以后的分析提供大量优质信号。一般来说，所有SQI都能有效识别严重失真的信号（R2组），准确率超过80%，其中大多数（SVSD, SDNN, RMSSD和SDSD）超过88%。但是，SQI在验证R1组的质量时有所不同。大多数SQI的准确率仅为60-65%。只有一个SQI（CVSD）达到70%，而表现最差的SQI（心率标准差）只有50%的准确性。然而，重要的是，在保留高质量信号方面，所有SQI都表现良好，保留了大约90%的有效信号。

在表3中描述的组合SQI的情况下，被拒绝的案例明显更高

10个最成功的组合在R2组中检测到超过90%的无效信号。对于R1组，拒绝的病例增加，所有组合的准确率均超过70%，其中一个组合的准确率约为80%。然而，这种性能的提高是以高质量组的准确率下降为代价的，准确率从89%下降到83%。值得注意的是，第二无效组中的丢弃率高于第一无效组中的丢弃率，这反映了第二组中的信号更加失真的事实。

检查错误分类的情况下，PPG信号的波形形态与标准PPG不完全匹配，因为舒张峰不明显。值得注意的是，这些仍然具有实用性，因为心率可以

TABLE 3 Performance of the best 10 combinations in classifying the good-quality segment.

Rule	Good accuracy	R1 accuracy	R2 accuracy	Accuracy	Brier	Roc	Fbeta
Entropy STD + CVSD	0.8978	0.7381	0.971	0.799	0.1264	0.8467	0.8785
MSQ + CVSD	0.8489	0.7762	1	0.7651	0.1552	0.8402	0.8604
Entropy + CVSD	0.8367	0.7905	1	0.7557	0.162	0.839	0.8569
SDNN + CVSD	0.8967	0.719	0.9565	0.7964	0.1315	0.8372	0.8729
Kurtosis mean + CVSD	0.9044	0.7095	0.942	0.8007	0.1281	0.8357	0.8747
Correlogram + CVSD	0.8933	0.719	0.9565	0.7939	0.134	0.8356	0.8709
RMSSD + CVSD	0.9	0.7143	0.942	0.7973	0.1306	0.8353	0.873
Zero crossing rate + CVSD	0.9033	0.7095	0.942	0.7998	0.1289	0.8352	0.8741
Kurtosis median + CVSD	0.9033	0.7095	0.942	0.7998	0.1289	0.8352	0.8741
CVSD + CVNNI	0.9033	0.7095	0.942	0.7998	0.1289	0.8352	0.8741

still be calculated from these as it is still feasible to identify the start and the end of a cycle. This observation is supported by the fact that the selected waveform focuses on per segment, which is not different in this case and resulted in the score of per segment surpassing the threshold. Finally, the use of a very small cutoff quantile indicates the superiority of the selected SQI and feasibility of this package.

In terms of validating the implementation, our package is limited as the original descriptions validated individual SQIs in diverse datasets. Consequently, each group of SQIs had a specific and different approach to validation. As the statistical SQI group is based on statistics algorithms (eg, skewness and kurtosis), these can be sufficiently validated by computing the values correctly on standard distributions. With HRV-based SQIs, were validated by comparing the values computed from other packages (R-HRV and HRV analyses). For the case of waveform-based and RR interval-based SQIs, the validities were evaluated by comparing a sequence of standard waveforms and the same sequence with additive noise.

4 Conclusion

The vital-sqi package has been carefully designed to assist health researchers of different backgrounds in carrying out SQI evaluation. The package provides an end-to-end solution from preprocessing to estimation of SQI scores and definitions of the quality of any ECG and PPG segments. This package concentrates on the estimation of various SQIs; yet, it is also flexible for users with different aims, enabling derivation of HRV features, pre-processing of data or detection of peaks.

Our experiment indicates the feasibility of categorizing the valid signals using the package. Instead of requiring users' deep domain knowledge, the package provides a simple-to-use pipeline with pre-search thresholds for the classification of invalid signals.

Furthermore, this package also allows users to define SQI rules. The good results described on a real-world dataset indicate the feasibility of the package as applying for other clinical trial setup.

The future work maintains the package up-to-date with modern SQIs and enhances the user interface. Although some SQIs describe the characteristics of the waveform or part of the segment, later versions of the package do not redirect to any vital sign analysis. Instead, the package will cooperate with other well-known libraries such as HeartPy or HRV analysis to retrieve the user needs.

Data availability statement

The datasets presented in this study can be found in online repositories. The names of the repository/repositories and accession number(s) can be found at: <https://pypi.org/project/vital-sqi/>.

Author contributions

Conceptualization, V-KL, HH, SK, BH, LT, HG, DC, and PG; formal analysis, V-KL, HH, and SK; funding acquisition, LT and DC; methodology, V-KL, HH, SK, BH, and DC; supervision, LT, DC, and PG; writing—original draft, V-KL, LT and HH; writing—review and editing, LT, DC, and PG; data collection, LT, VHN, NQKP and TPL; data annotation, NQKP. All authors have read and agreed to the published version of the manuscript.

Funding

This research was supported by the Wellcome Trust under grant WT217650/Z/19/Z. D.A.C was supported in part by the National Institute for Health Research (NIHR) Oxford Biomedical Research Centre; an InnoHK Project at the Hong Kong Centre for Cerebro-cardiovascular Health Engineering; and the Pandemic Sciences Institute, University of Oxford, Oxford, United Kingdom.

表3在对高质量段进行分类时最佳10种组合的性能。

Rule	良好的精度	R1准确度	R2准确度	精度	Brier	Roc	Fbeta
熵STD + CVSD	0.8978	0.7381	0.971	0.799	0.1264	0.8467	0.8785
MSQ + CVSD	0.8489	0.7762	1	0.7651	0.1552	0.8402	0.8604
熵+ CVSD	0.8367	0.7905	1	0.7557	0.162	0.839	0.8569
SDNN + CVSD	0.8967	0.719	0.9565	0.7964	0.1315	0.8372	0.8729
峰度均值+ CVSD	0.9044	0.7095	0.942	0.8007	0.1281	0.8357	0.8747
相关图+ CVSD	0.8933	0.719	0.9565	0.7939	0.134	0.8356	0.8709
RMSSD + CVSD	0.9	0.7143	0.942	0.7973	0.1306	0.8353	0.873
过零率+ CVSD	0.9033	0.7095	0.942	0.7998	0.1289	0.8352	0.8741
峰度中位数+ CVSD	0.9033	0.7095	0.942	0.7998	0.1289	0.8352	0.8741
CVSD + CVNNI	0.9033	0.7095	0.942	0.7998	0.1289	0.8352	0.8741

仍然可以从这些计算，因为它仍然是可行的，以确定一个周期的开始和结束。该观察结果得到以下事实的支持：所选波形关注每个分段，在这种情况下没有不同，并且导致每个分段的分数超过阈值。最后，使用一个非常小的截断分位数表明所选择的SQI的优越性和该软件包的可行性。

在验证实现方面，我们的包是有限的，因为原始描述在不同的数据集中验证了单个SQI。因此，每组SQI都有一个特定的和不同的验证方法。由于统计SQI组基于统计算法（例如，偏度和峰度），这些可以通过在标准分布上正确地计算值来充分验证。通过比较其他软件包（R-HRV和HRV分析）计算的值，对基于HRV的SQIs进行了验证。对于基于波形和基于RR intervalbased SQI的情况，通过比较标准波形序列和具有加性噪声的相同序列来评估有效性。

未来的工作保持包最新的现代SQIs和增强用户界面。尽管一些SQI描述了波形或部分片段的特征，但软件包的后续版本不会重定向到任何生命体征分析。相反，该软件包将与HeartPy或HRV分析等其他知名库合作，以检索用户需求。

数据可用性声明

本研究中提供的数据集可以在在线存储库中找到。储存库名称和登录号可在<https://pypi.org/project/vital-sqi/>上找到。

作者贡献

概念化，V-KL、HH、SK、BH、LT、HG、DC和PG;形式分析，V-KL、HH和SK;资金获取，LT和DC;方法学，V-KL、HH、SK、BH和DC;监督，LT、DC和PG;撰写-原始草案，V-KL、LT和HH;撰写-审查和编辑，LT、DC和PG;数据收集，LT、VHN、NQKP和TPL;数据注释，NQKP。所有作者均已阅读并同意手稿的出版版本。

4结论Vital-SQI软件包经过精心设计，可以帮助不同背景的健康研究者进行SQI评价。该软件包提供了一个端到端的解决方案，从预处理到SQI评分的估计以及任何ECG和PPG段质量的定义。该软件包专注于各种SQI的估计；然而，对于具有不同目标的用户来说，它也是灵活的，可以导出HRV特征，预处理数据或检测峰值。

实验结果表明，该软件包对有效信号进行分类是可行的。该软件包提供了一个简单易用的管道，带有用于分类无效信号的预设阈值，而不需要用户的深入领域知识。

资金

这项研究得到了Wellcome Trust的资助，资助号为WT 217650/Z/19/Z。D.A.C.得到英国国家卫生研究院（NIHR）牛津生物医学研究中心、香港心脑血管健康工程中心的一个创新香港项目，以及英国牛津大学流行病科学研究所的部分支持。

此外，该软件包还允许用户定义SQI规则。

在真实世界数据集上描述的良好结果表明该软件包适用于其他临床试验设置的可行性。

Acknowledgments

We would like to thank the **Vietnam ICU Translational Applications Laboratory (VITAL) investigators, OUCRU inclusive authorship list in Vietnam** (alphabetic order by surname): Dang Phuong Thao, Dang Trung Kien, Doan Bui Xuan Thy, Dong Huu Khanh Trinh, Du Hong Duc, Ronald Geskus, Ho Bich Hai, Ho Quang Chanh, Ho Van Hien, Huynh Trung Trieu, Evelyne Kestelyn, Lam Minh Yen, Le Dinh Van Khoa, Le Thanh Phuong, Le Thuy Thuy Khanh, Luu Hoai Bao Tran, Luu Phuoc An, Angela McBride, Nguyen Lam Vuong, Ngan Nguyen Lyle, Nguyen Quang Huy, Nguyen Than Ha Quyen, Nguyen Thanh Ngoc, Nguyen Thi Giang, Nguyen Thi Diem Trinh, Nguyen Thi Le Thanh, Nguyen Thi Phuong Dung, Nguyen Thi Phuong Thao, Ninh Thi Thanh Van, Pham Tieu Kieu, Phan Nguyen Quoc Khanh, Phung Khanh Lam, Phung Tran Huy Nhat, Guy Thwaites, Louise Thwaites, Tran Minh Duc, Trinh Manh Hung, Hugo Turner, Jennifer Ilo Van Nuil, Vo Tan Hoang, Vu Ngo Thanh Huyen, Sophie Yacoub, **Hospital for Tropical Diseases, Ho Chi Minh City** (alphabetic order by surname): Cao Thi Tam, Duong Bich Thuy, Ha Thi Hai Duong, Ho Dang Trung Nghia, Le Buu Chau, Le Mau Toan, Le Ngoc Minh Thu, Le Thi Mai Thao, Luong Thi Hue Tai, Nguyen Hoan Phu, Nguyen Quoc Viet, Nguyen Thanh Dung, Nguyen Thanh Nguyen, Nguyen Thanh Phong, Nguyen Thi Kim Anh, Nguyen Van Hao, Nguyen Van Thanh Duoc, Pham Kieu Nguyet Oanh, Phan Thi Hong Van, Phan Tu Qui, Phan Vinh Tho, Truong Thi Phuong Thao, **University of Oxford** (alphabetic order by surname): Natasha Ali, David Clifton, Mike English, Jannis Hagenah, Ping Lu, Jacob McKnight, Chris Paton, Tingting Zhu, **Imperial College London** (alphabetic order by surname): Pantelis Georgiou, Bernard Hernandez Perez, Kerri Hill-Cawthorne, Alison Holmes, Stefan Karolcik, Damien Ming, Nicolas Moser, Jesus Rodriguez Manzano, **King's College London**

References

- Akbilgic, O., Butler, L., Karabayir, I., Chang, P. P., Kitzman, D. W., Alonso, A., et al. (2021). ECG-AI: Electrocardiographic artificial intelligence model for prediction of heart failure. *Eur. Heart J. Digit. Health* 2, 626–634. doi:10.1093/ehjdh/ztab080
- Badawi, A. A., Badr, A., and Elgazzar, K. (2021). “Ecg real-time monitoring and heart anomaly detection reimaged,” in 2021 IEEE 7th World Forum on Internet of Things (WF-IoT), 326–331. doi:10.1109/WF-IoT51360.2021.9595639
- Becker, D. (2006). Fundamentals of electrocardiography interpretation. *Anesth. Prog.* 53, 53–63. quiz 64. doi:10.2344/0003-3006(2006)53[53:FOEI]2.0.CO;2
- Billauer, E. (2009). *peakdet: Peak detection using matlab. my tech blog* Accessed: 2022-12-05.
- Elgendi, M., Norton, I., Brearley, M., Abbott, D., and Schuurmans, D. (2013). Systolic peak detection in acceleration photoplethysmograms measured from emergency responders in tropical conditions. *PLoS ONE* 8, 76585. doi:10.1371/journal.pone.0076585
- Elgendi, M. (2012). On the analysis of fingertip photoplethysmogram signals. *Curr. Cardiol. Rev.* 8, 14–25. doi:10.2174/157340312801215782
- Elgendi, M. (2016). Optimal signal quality index for photoplethysmogram signals. *Bioengineering* 3, E21. doi:10.3390/bioengineering3040021
- Krishnan, R., Natarajan, B., and Warren, S. (2010). Two-stage approach for detection and reduction of motion artifacts in photoplethysmographic data. *IEEE Trans. Biomed. Eng.* 57, 1867–1876. doi:10.1109/TBME.2009.2039568
- Lee, J., Kim, M., Park, H.-K., and Kim, I. Y. (2020). Motion artifact reduction in wearable photoplethysmography based on multi-channel sensors with multiple wavelengths. *Sensors (Basel)* 20, 1493. doi:10.3390/s20051493
- Li, Q., and Clifford, G. D. (2012). Dynamic time warping and machine learning for signal quality assessment of pulsatile signals. *Physiol. Meas.* 33, 1491–1501. doi:10.1088/0967-3334/33/9/1491
- Marco, L., Duan, W., Bojarnejad, M., Zheng, D., King, S., Murray, A., et al. (2012). Evaluation of an algorithm based on single-condition decision rules for binary classification of 12-lead ambulatory ecg recording quality. *Physiol. Meas.* 33, 1435–1448. doi:10.1088/0967-3334/33/9/1435
- Nagai, S., Anzai, D., and Wang, J. (2017). Motion artefact removals for wearable ECG using stationary wavelet transform. *Healthc. Technol. Lett.* 4, 138–141. doi:10.1049/htl.2016.0100
- Nantume, A., Shah, S., Cauvel, T., Tomback, M., Kilpatrick, R., Afzal, B., et al. (2021). Developing medical technologies for low-resource settings: Lessons from a wireless wearable vital signs monitor-neoGuard. *Front. Digit. Health* 3, 730951. doi:10.3389/fdgh.2021.730951
- Orphanidou, C., Bonnici, T., Charlton, P., Clifton, D., Vallance, D., and Tarassenko, L. (2014). Signal-quality indices for the electrocardiogram and photoplethysmogram: Derivation and applications to wireless monitoring. *IEEE J. Biomed. Health Inf.* 19, 832–838. doi:10.1109/JBHI.2014.2338351

(alphabetic order by surname): Liane Canas, Alberto Gomez, Hamideh Kerdegari, Andrew King, Marc Modat, Reza Razavi, Miguel Xochicale, **University of Ulm** (alphabetic order by surname): Walter Karlen, **The University of Melbourne** (alphabetic order by surname): Linda Denehy, Thomas Rollinson, and **Mahidol Oxford Tropical Medicine Research Unit (MORU)** (alphabetic order by surname): Luigi Pisani, Marcus Schultz.

Conflict of interest

The authors declare that the research was conducted in the absence of any commercial or financial relationships that could be construed as a potential conflict of interest.

Publisher's note

All claims expressed in this article are solely those of the authors and do not necessarily represent those of their affiliated organizations, or those of the publisher, the editors, and the reviewers. Any product that may be evaluated in this article, or claim that may be made by its manufacturer, is not guaranteed or endorsed by the publisher.

Supplementary material

The Supplementary Material for this article can be found online at: <https://www.frontiersin.org/articles/10.3389/fphys.2022.1020458/full#supplementary-material>

致谢

我们要感谢越南ICU翻译

应用实验室（VITAL）研究者，OUCRU（包括越南的作者名单）
 （按姓氏字母顺序排列）：Dang Dong Thao, Dang Trung Kien, 多安Bui Xuan Thy, Dong Huu Khanh Trinh, Du Hong Duc, 罗纳德Geskus, Ho Bich Hai, Ho Quang Chanhan, Ho货车Hien, Huynh Trung Trieu, Evelyne Kestelyn, Lam Minh Yen, Le Dinh货车Khoa, Le Thanh Dong, Le Thuy Thuy Khanh, Luu Hoai Bao Tran, Luu Jioc An, Angela McBride, Nguyen Lam Vuong, Ngan Nguyen Lyle, Nguyen Quang胡伊, Nguyen Than Ha Quyen, Nguyen Thanh Ngoc, Nguyen Thi Giang, Nguyen Thi Diem Trinh, Nguyen Thi Le Thanh, Nguyen Thi Jiong Dung, Nguyen Thi Jiong Thao, Ninh Thi Thanh货车, Pham Tieu Kieu, Phan Nguyen Quoc Khanh, Phung Khanh Lam, Phung Tran胡伊Nhat, Guy Thwaites, Louise Thwaites, Tran Minh Duc, Trinh Manh Hung, Hugo Turner, Jennifer Ilo货车Nuil, Vo Tan Hoang, Vu Ngo Thanh Huyen, Sophie Yacoub, 热带病医院, 胡志明市（按姓氏字母顺序）：Cao Thi Tam, Duong Bich Thuy, Ha Thi Hai 杨丽萍, 吴丽萍, 吴丽萍牛津大学（字母顺序姓氏）：娜塔莎·阿里, 大卫·克利夫顿, 迈克·英格利希, 詹尼斯·哈根纳, 卢平, 雅各布·麦克奈特, 克里斯·佩顿, 庭庭朱, 伦敦帝国理工学院（按字母顺序姓氏）：潘特利斯·乔治欧伯纳德·埃尔南德斯·佩雷斯凯里·希尔·考索恩艾莉森·霍姆斯斯特凡·卡罗西克达米安·明尼古拉斯·莫泽

伦敦国王学院（按姓氏字母顺序）：Liane Canas, Alberto Gomez, Hamideh Kerdegari, Andrew King, Marc Modat, Reza Razavi, Miguel Xochicale, 乌尔姆大学（按姓氏字母顺序排列）：沃尔特·卡伦, 墨尔本大学（按姓氏字母顺序排列）：琳达德尼、托马斯罗林森和玛希多尔牛津热带医学研究所（MORU）（按姓氏字母顺序排列）：路易吉·皮萨尼, 马库斯·舒尔茨。

利益冲突

作者声明，本研究是在不存在任何可能被视为潜在利益冲突的商业或财务关系的情况下进行的。

出版者的笔记

本文中表达的所有主张仅代表作者，不一定代表其附属组织，或出版商，编辑和评审员。本文中可能评估的任何产品，或其制造商可能提出的任何声明，均不受出版商的担保或认可。

补充材料

这篇文章的补充材料可以在网上找到：

<https://www.frontiersin.org/articles/10.3389/fphys.2022.1020458/full#材料>

参考文献

- ”他, O. 巴特勒, L. 卡拉马, I. 张, P. 基兹曼, D. W. Alonso A来吧 (2021年)。ECG-AI: 用于预测心力衰竭的心电图人工智能模型。EUR. Heart J. Digit. 健康2, 626-634. doi: 10.1093/ehjdh/ztab080
- Badawi, A.一、Badr, A., Elgazzar, K. (2021年)。“ECG 实时监测和心脏异常检测重新构想”, 2021年IEEE第7届世界物联网论坛 (WF-IoT) , 326-331. doi: 10.1109/WF-IoT51360.2021.9595639
- Becker, D. (2006年)。心电图判读基础。麻醉Prog. 53, 53-63。小测验64. doi: 10.2344/0003-3006 (2006) 53[53: FOEI]2.0.CO;2
- Billauer, E. (2009年)。peakdet: 使用matlab进行峰值检测。我的技术博客访问: 2022-12-05. Elgendi, M., 诺顿岛, 布里尔利, M., Abbott, D., 和Schuurmans, D. (2013年)。在紧急情况下测量的加速度光电容积描记图中的收缩压峰值检测。PLoS ONE 8, 765855. doi: 10.1371/journal.pone.0076585
- Elgendi, M. (2012年)。指尖光电容积图信号的分析。Curr. Cardiol. Rev. 8, 14-25. 手机: 157340312801215782
- Elgendi, M. (2016年)。光电容积描记图信号的最佳信号质量指标。生物工程3, E21. doi: 10.3390/bioengineering3040021
- 克里希南河, Natarajan, B., 和Warren, S. (2010年)。光电容积描记数据中运动伪影检测和减少的两阶段方法。IEEE 生物医学学报Eng. 57, 1867-1876. doi: 10.1109/TBME.2009.2039568
- 李, J., Kim, M., 帕克, H.-K., 金, 我, Y. (2020年)。基于具有多个波长的多通道传感器的可穿戴光电容积描记中的运动伪影减少。传感器 (巴塞尔) 20, 1493. doi: 10.3390/s20051493
- 李, Q., Clifford, G. D. (2012年)。动态时间规整和机器学习用于脉动信号的信号质量评估。生理学测量33, 1491-1501. doi: 10.1088/0967-3334/33/9/1491
- 马可湖段伟, Bojarnejad, M., Zheng, D., King, S., Murray, A., 等 (2012年)。基于单条件决策规则的12导联动态心电图记录质量二元分类算法的评价。生理学测量33, 1435-1448. doi: 10.1088/0967-3334/33/9/1435
- 永井, S., Anzai, D., Wang, J. (2017) .基于平稳小波变换的穿戴式心电图运动伪影去除方法。保健c.技术信函4, 138-141. doi: 10.1049/htl.2016.0100
- Nantume, A., Shah, S., Cauvel, T., Tomback, M., 基尔帕特里克河, Afzal, B., 等 (2021年)。为低资源环境开发医疗技术: 从无线可穿戴vitalsignsmonitor-neoGuard的教训。前。数字。健康3, 730951. doi: 10.3389/fdgth.2021.730951
- Orphanidou角, Bonnici, T., 查尔顿, P., 克利夫顿博士, Vallance, D., 和Tarassenko, L. (2014年)。心电图和光电容积描记图的信号质量指数: 推导和无线监测的应用。IEEE J. Biomed. Health Inf. 19, 832-838. doi: 10.1109/JBHI.2014.2338351

- Pereira, T., Tran, N., Gadhumi, K., Pelter, M. M., Do, D. H., Lee, R. J., et al. (2020). Photoplethysmography based atrial fibrillation detection: A review. *NPJ Digit. Med.* 3, 3. doi:10.1038/s41746-019-0207-9
- Pollreisz, T. N., D., and TaheriNejad, N. (2022). Detection and removal of motion artifacts in ppg signals. *Mob. Netw. Appl.* 27, 728–738. doi:10.1007/s11036-019-01323-6
- Pradhan, N., Rajan, S., Adler, A., and Redpath, C. (2017). “Classification of the quality of wristband-based photoplethysmography signals,” in 2017 IEEE International Symposium on Medical Measurements and Applications (MeMeA), 269–274. doi:10.1109/MeMeA.2017.7985887
- Raghunath, S., Ulloa Cerna, A. E., Jing, L., vanMaanen, D. P., Stough, J., Hartzel, D. N., et al. (2020). Prediction of mortality from 12-lead electrocardiogram voltage data using a deep neural network. *Nat. Med.* 26, 886–891. doi:10.1038/s41591-020-0870-z
- Champseix, R. (2018). HRV analysis: Heart rate variability analysis. Available at: <https://github.com/Aura-healthcare/hrv-analysis> (Accessed March 14, 2022).
- Sana, F., Isselbacher, E. M., Singh, J. P., Heist, E. K., Pathik, B., and Armoundas, A. A. (2020). Wearable devices for ambulatory cardiac monitoring: JACC state-of-the-art review. *J. Am. Coll. Cardiol.* 75, 1582–1592. doi:10.1016/j.jacc.2020.01.046
- Schäfer, A., and Kratky, K. (2008). Estimation of breathing rate from respiratory sinus arrhythmia: Comparison of various methods. *Ann. Biomed. Eng.* 36, 476–485. doi:10.1007/s10439-007-9428-1
- Selvaraj, N., Mendelson, Y., Shelley, K. H., Silverman, D. G., and Chon, K. H. (2011). Statistical approach for the detection of motion/noise artifacts in Photoplethysmogram. *Annu. Int. Conf. IEEE Eng. Med. Biol. Soc.* 2011, 4972–4975. doi:10.1109/IEMBS.2011.6091232
- Seok, D., Lee, S., Kim, M., Cho, J., and Kim, C. (2021). Motion artifact removal techniques for wearable eeg and ppg sensor systems. *Front. Electron.* 2. doi:10.3389/felc.2021.685513
- Shin, H. S., Lee, C., and Lee, M. (2009). Adaptive threshold method for the peak detection of photoplethysmographic waveform. *Comput. Biol. Med.* 39, 1145–1152. doi:10.1016/j.combiomed.2009.10.006
- Tadesse, G. A., Zhu, T., Le Nguyen Thanh, N., Hung, N. T., Duong, H. T. H., Khanh, T. H., et al. (2020). Severity detection tool for patients with infectious disease. *Healthc. Technol. Lett.* 7, 45–50. doi:10.1049/htl.2019.0030
- van Gent, P., Farah, H., van Nes, N., and van Arem, B. (2019). Analysing noisy driver physiology real-time using off-the-shelf sensors: Heart rate analysis software from the taking the fast lane project. *J. Open Res. Softw.* 7 (1), 32. doi:10.5334/jors.241
- van Gent, P., Farah, H., van Nes, N., and van Arem, B. (2019). HeartPy: A novel heart rate algorithm for the analysis of noisy signals. *Transp. Res. F: Traffic Psychol. Behav.* 66, 368–378. doi:10.1016/j.trf.2019.09.015
- Virtanen, P., Gommers, R., Oliphant, T. E., Haberland, M., Reddy, T., Cournapeau, D., et al. (2020). SciPy 1.0: Fundamental algorithms for scientific computing in Python. *Nat. Methods* 17, 261–272. doi:10.1038/s41592-019-0686-2
- Zong, W., Heldt, T., Moody, G., and Mark, R. (2003). An open-source algorithm to detect onset of arterial blood pressure pulses. *Comput. Cardiol.* 30, 259–262. doi:10.1109/CIC.2003.1291140

- 佩雷拉, T., Tran, N., Gadhouni, K., Pelter, M. M., 多, D. H.、利河, 巴西-地J., 等人(2020年)。基于光电体积描记术的房颤检测: 综述。NPJ数字Med. 3, 3. doi: 10.1038/s41746-019-0207-9
- Pollreisz, T. N., D. 和 TaheriNejad, N. (2022年)。ppg信号中运动伪影的检测与去除。暴徒网络Appl. 27, 728-738. doi: 10.1007/s11036-019-01323-6
- Pradhan, N., Rajan, S., Adler, A., 和 Redpath, C. (2017年)。“基于腕带的光电体积描记信号的质量分类”, 2017年IEEE 国际医学测量和应用研讨会(MeMeA), 269-274. doi: 10.1109/MeMeA.2017.7985887
- Raghunath, S., Ulloa Cerna, A. E., Jing, L., vanMaanen, D. P., Stough, J., Hartzel, D. N., 等(2020年)。使用深度神经网络从12导联心电图电压数据预测死亡率。26, 886-891. doi: 10.1038/s41591-020-0870-z
- 尚普塞河(2018年)。HRV分析: 心率变异性分析。
网址: <https://github.com/Aura-healthcare/hrv-analysis> (2022年3月14日访问)。
- Sana, F., Isselbacher, E. M., Singh, J.P. 海斯特, E. K., Pathik, B., 和 Armoundas, A. A. (2020年)。用于动态心脏监测的可穿戴设备: JACC最新技术综述。J. Am. 胶原心脏 75, 1582-1592. doi: 10.1016/j.jacc.2020.01.046
- Schäfer, A., Kratky, K. (2008年)。呼吸性窦性心律失常的呼吸频率估计: 各种方法的比较。安. 生物医学。Eng. 36, 476-485. doi: 10.1007/s10439-007-9428-1
- 光电容积描记图。Annu.国际会议IEEE 工程医学生物学会, 2011年, 4972-4975. doi: 10.1109/IEMBS.2011.6091232
- Seok, D., 李, S., Kim, M., 周, J., 和 Kim, C. (2021年)。可穿戴eeg和ppg传感器系统的运动伪影去除技术。前面电子2. doi: 10.3389/felec.2021.685513
- 申, H.美国, 李, C., 和 Lee, M. (2009年)。光电容积脉搏波峰值检测的自适应阈值方法。Comput.生物医学39, 1145-1152. doi: 10.1016/j.combiomed.2009.10.006
- Tadesse, G.-、Zhu, T., Le Nguyen Thanh, N., Hung, N. T., Duong, H. T. H., Khanh, T. H. 等(2020年)。传染病患者严重程度检测工具。保健c.技术信7, 45-50。版权所有© 2019 - 2019 www.jsjsj.com
- 货车Gent, P., 法拉, H., 货车内斯, 和货车Arem, B. (2019年)。使用现成的传感器实时分析嘈杂的驾驶员生理学: 来自快车道项目的心率分析软件。J. Open Res. Softw. 7 (1), 32. doi: 10.5334/jors.241
- 货车Gent, P., 法拉, H., 货车内斯, 和货车Arem, B. (2019年)。HeartPy: 一种用于分析噪声信号的新型心率算法。运输单研究F: 交通心理行为。66, 368-378. doi: 10.1016/j.trf.2019.09.015
- 维尔塔宁, P., 戈默斯河, Oliphant, T. E.、Haberland, M., Reddy, T., Cournapeau, D., 等(2020年)。SciPy 1.0: Python中科学计算的基本算法。Nat. Methods 17, 261-272. doi: 10.1038/s41592-019-0688-2
- Zong, W., Heldt, T., 穆迪, G., 和Mark, R. (2003年) 的报告。一个开源算法来检测动脉血压脉搏的开始。Comput. Cardiol. 30, 259-262. doi: 10.1109/CIC.2003.1291140

Selvaraj, N., Mendelson, Y., Shelley, K. H. 西尔弗曼, D. G., 和 Chon, K. H. (2011年)。运动/噪声伪影检测的统计方法